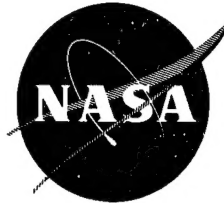


0420079

SK1

NASA CR-134720

AMS Report No. 1141



181

Princeton University

ANALYSIS OF EDGE IMPACT STRESSES IN COMPOSITE PLATES

by F. C. Moon, C. K. Kang
Princeton University, Princeton, N. J.

prepared for
NATIONAL AERONAUTICS AND SPACE ADMINISTRATION
Washington, D. C. 20546

NASA Lewis Research Center, Cleveland, Ohio 44135
Contract NGR 31-001-267

Topical Report
May 1973 to May 1974

DISTRIBUTION STATEMENT A

Approved for public release
Distribution Unlimited



19960206 138

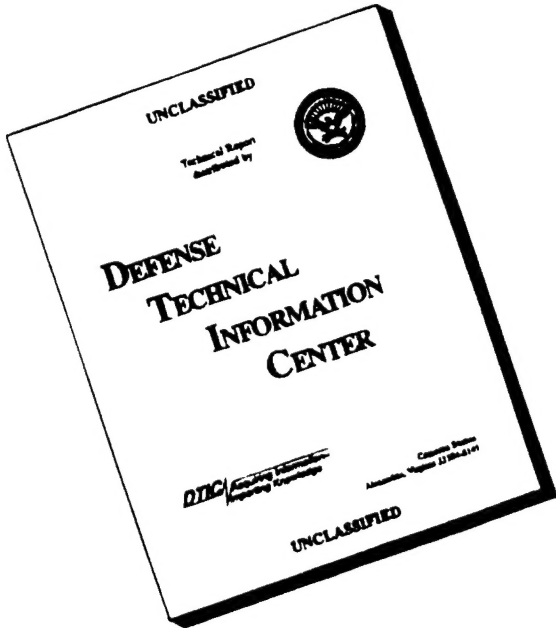
PRINCETON
UNIVERSITY

Department of
Aerospace and
Mechanical Sciences

20508

DTIC QUALITY INSPECTED

DISCLAIMER NOTICE



THIS DOCUMENT IS BEST
QUALITY AVAILABLE. THE
COPY FURNISHED TO DTIC
CONTAINED A SIGNIFICANT
NUMBER OF PAGES WHICH DO
NOT REPRODUCE LEGIBLY.

1. Report No. NASA CR-134720	2. Government Accession No.	3. Recipient's Catalog No.	
4. Title and Subtitle Analysis of Edge Impact Stresses in Composite Plates		5. Report Date July 1974	
7. Author(s) F. C. Moon, C. K. Kang		6. Performing Organization Code	
9. Performing Organization Name and Address Princeton University Princeton, NJ 08540		8. Performing Organization Report No. AMS Report No. 1141	
12. Sponsoring Agency Name and Address National Aeroanutics and Space Administration Washington, DC 20546		10. Work Unit No.	
15. Supplementary Notes Project Manager, C. C. Chamis Materials and Structures Division NASA-Lewis Research Center Cleveland, OH 44135		11. Contract or Grant No. NGR 31-001-267	
16. Abstract The in-plane edge impact of composite plates, with or without a protection strip, is investigated in this work. A computational analysis based on the Fast Fourier Transform technique is presented. The particular application of the present method is in the understanding of the foreign object damage problem of composite fan blades. However, the method is completely general and may be applied to the study of other stress wave propagation problems in a half space. Results indicate that for the protective strip to be effective in reducing impact stresses in the composite the thickness must be equal or greater than the impact contact dimension. Also large interface shear stresses at the strip - composite boundary can be induced under impact.		13. Type of Report and Period Covered Topical Report May 1973 to May 1974	
17. Key Words (Suggested by Author(s)) Fiber composite plates, high velocity impact, in-plane edge impact, edge protection, foreign object damage, displacement and stress waves, contact time, fast fourier transform, computer program		18. Distribution Statement Unclassified, unlimited	
19. Security Classif. (of this report) Unclassified	20. Security Classif. (of this page) Unclassified	21. No. of Pages 73	22. Price* \$3.00

* For sale by the National Technical Information Service, Springfield, Virginia 22151

ABSTRACT

The in-plane edge impact of composite plates, with or without a protection strip, is investigated in this work. A computational analysis based on the Fast Fourier Transform technique is presented. The particular application of the present method is in the understanding of the foreign object damage problem of composite fan blades. However, the method is completely general, and may be applied to the study of other stress wave propagation problems in a half space. Results indicate that for the protective strip to be effective in reducing impact stresses in the composite the thickness must be equal or greater than the impact contact dimension. Also large interface shear stresses at the strip - composite boundary can be induced under impact.

TABLE OF CONTENTS

	<u>Page</u>
Abstract	i
Table of Contents	ii
List of Tables	iii
List of Figures	iv, v
Introduction	1
I Basic equations for edge loading on an anisotropic plate	4
II Edge impact of plate with edge protection	11
III Numerical inversion	14
IV Results	20
Summary of results	23
References	24
Tables	25
Appendicies	
A. Determination of parameter C_0 in Laplace inversion	26
B. Flow chart of computer program	28
C. Notes on computer program	30
D. Program input and output.	32
Figures.	

LIST OF TABLES

	page
Table I Stress-Strain coefficients for 55% graphite fiber/epoxy matrix composite	25

LIST OF FIGURES*

1. Geometry of in-plane edge impact of a composite plate with a protection strip.
2. Body wave speeds and Rayleigh wave speed versus fiber lay-up angle for 55% graphite fiber in epoxy matrix.
3. Branches and singular points in the complex Laplace plane.
4. Rayleigh wave for stress t_{11} , impact time 35 μ sec, impact length 2 cm, 55% graphite fiber/epoxy matrix 0° lay-up angle - no strip.
5. Rayleigh wave for stress t_{11} , impact time 35 μ /sec, impact length 2 cm, 55% graphite fiber/epoxy matrix 15° lay-up angle.
6. Level computer map in x_1 - time plane for applied stress t_{33} , 0° LAY-UP ANGLE on $x_3 = 0$.
7. Level computer map in x_1 - time plane for stress wave t_{11} , 0° Lay-up angle on $x_3 = 0$.
8. Decrease of impact stress with distance from the impact edge.
9. Stress t_{33} versus time for normalized depths $x_3 = 0, 1, 2$.
10. Maximum impact stress levels versus layup angles for 55% graphite fiber/epoxy matrix composite.
11. Effect of layup angle on distribution of stress t_{33} versus x_1 at a normalized depth $x_2 = 1$ for 55% graphite fiber/epoxy matrix composite.
- 12a Effect of steel edge strip thickness on impact stresses at the strip edge interface for 55% graphite fiber/epoxy matrix composite, $\pm 15^\circ$ layup angle.
- 12b Effect of steel edge strip thickness on impact stresses at the strip edge interface for 55% graphite fiber/ **epoxy** matrix composite $\pm 45^\circ$ layup angle.
13. Effect of Aluminum edge strip thickness on impact stresses at the strip edge interface for 55% graphite fiber/epoxy matrix composite 0° layup angle.
14. Effect of steel edge strip thickness on t_{33} stress distribution versus along edge interface for normalized thicknesses $b/a = 0.1, 1.0, 55\%$ graphite fiber/epoxy matrix composite.

*Except for Figure 6, a contact time of 35 μ sec and contact length of 2 cm was used in these calculations.

15. Effect of steel edge strip thickness on t_{11} stress distribution versus along edge interface for normalized thicknesses $b/a = 0.1, 1.0, 55\%$ graphite fiber/epoxy matrix composite.
16. Effect of steel edge strip thickness on edge interface shear stress distribution for normalized edge thickness $b/a = 0.25, 2.0, 55\%$ graphite fiber/epoxy matrix composite.

INTRODUCTION

This report is part of a continuing effort by NASA to understand the basic mechanics of foreign object impact of composite materials of particular interest are damage resistant designs of jet engine fan blades under hail or bird impact. In previous reports the central or normal impact response of composite plates was examined [1]. In this report the mechanics of edge impact of composite plates are examined. This is schematically illustrated in Figure 1.

The basic approach to the study of impact of composite plates in this program has been to examine the stress waves generated by the impact forces. For central impact of plates it has been shown that in addition to wave propagation across the plate thickness, bending and extensional waves propagate away from the impact site. The stresses associated with these waves have been studied without considering the effect of boundaries such as the free or clamped edges of a fan blade. This simplification has been made on the premise that for short impact times e.g. less than 10^{-4} sec. few edge reflections have taken place, and that the highest stresses occur at the impact site. However, for edge impact, the boundary conditions greatly affect the nature of the wave mechanics.

Edge waves in solids have been studied extensively in seismology. The principal phenomenon is the entrapment of wave energy in a layer near the surface. This surface wave is known as a Rayleigh wave and travels at a velocity below the shear velocity for isotropic solids. For plates, however, two types of edge waves can occur as shown in Figure 2a. For impact transverse to the plate, flexural edge waves can occur. For in-plane, Rayleigh type edge waves are generated. In this report only in-plane edge waves will be discussed.

Wave type solutions to the equations of elastodynamics of an orthotropic plate which exponentially decay away from the edge (X_3 direction) and propagate along the edge (X_1 direction) can be found provided the edge wave velocity satisfies the equation (Reference 9).

$$\rho v^2 + \left[\frac{C_{55} - \rho v^2}{\frac{C_{33} C_{55} (C_{11} - \rho v^2)}{C_{13} C_{33} C_{11}}} \right]^{1/2} [C_{13}^2 - C_{33} (C_{11} - \rho v^2)] = 0$$

where ρ is the massdensity of the plate and C_{ij} are the effective plate elastic constants (denoted by \hat{C}_{ij} in Reference 1). It can be shown that one real root lies in the interval

$$0 < \rho v^2 < C_{55}$$

Thus, the edge or Rayleigh wave speed is less than the shear speed in this direction $[C_{55} / \rho]^{1/2}$.

Changing the layup angle will affect the elastic constants C_{ij} and hence, change the value of the edge wave velocity. The results of this calculation are shown in Figure 2b where the C_{ij} are obtained from Reference 7. The edge wave speed seems to obtain a maximum between ± 15 and $\pm 30^\circ$ layup angle which is below the extentional wave speeds labelled "dilational" and "shear" in Figure 2b and which is greater than the bending wave velocity.

In order to prevent damage to composite fan blades under foreign object impact leading edge protection has been used. (See e.g. Ref. (8)). This usually consists of a strip of metal attached to the leading edge of the fan blade. To model the effects of this impact protection strip, the in-plane edge impact of an anisotropic plate, with a beam-strip attached to the impact edge, has been studied (see Figure 1). It will be shown later that the strip will decrease the tensile stress along the edge while producing shear stress between the strip and the plate edge.

I. BASIC EQUATIONS FOR EDGE LOADING ON ANISOTROPIC PLATE

Let the plate be the half-space $x_3 > 0$. The equations of motion are given by [1] as:

$$C_{11} u_{1,11} + C_{55} u_{1,33} + (C_{13} + C_{55}) u_{3,13} = \rho u_{1,tt} \quad (1.1)$$

$$C_{33} u_{3,33} + C_{55} u_{3,11} + (C_{13} + C_{55}) u_{1,13} = \rho u_{3,tt}$$

here we have employed $C_{11}, C_{13}, C_{33} \dots$ to denote $\hat{C}_{11}, \hat{C}_{13}, \hat{C}_{33} \dots$ of [1]. The in-plane motion is assumed to be independent of the bending deformation. With the loading condition shown in Figure 1, the boundary conditions are (without protection strip):

$$t_{13}(x_1, 0, t) = C_{55}(u_{1,3} + u_{3,1}) \Big|_{x_3=0} = 0 \quad (1.2)$$

$$t_{33}(x_1, 0, t) = [C_{33} u_{3,3} + C_{13} u_{1,1}] \Big|_{x_3=0} = p f(x_1) g(t)$$

The following nondimensional parameters are used;

$$C_{11}^* = C_{11}/C_{66}, \quad C_{13}^* = C_{13}/C_{66}, \quad C_{33}^* = C_{33}/C_{66}, \quad C_{55}^* = C_{55}/C_{66}, \quad P_0^* = p/C_{66} \quad (1.3)$$

$$u_1^* = u_1/\ell, \quad u_3^* = u_3/\ell, \quad x_1^* = x_1/\ell, \quad x_3^* = x_3/\ell, \quad t^* = t \sqrt{C_{66}/\rho}/\ell \quad (1.4)$$

ℓ is a length parameter. C_{66} is a typical elastic constant. In what follows the equations will be assumed to be nondimensionalized using (1.3) and (1.4).

To obtain the solution, we employ transform methods. Define:

$$F(f) = \frac{1}{2\pi} \int_{-\infty}^{\infty} e^{-ik_1 x_1} f(x_1) dx_1$$

as the Fourier transform of $f(x)$ where we assume that

$$f(x_1) \Big|_{-\infty}^{\infty} = \frac{\partial}{\partial x_1} f(x_1) \Big|_{-\infty}^{\infty} = 0$$

Then

$$F\left(\frac{\partial}{\partial x_1} f\right) = ik_1 F(f), \quad F\left(\frac{\partial^2}{\partial x_1^2} f\right) = -k_1^2 F(f)$$

Also define

$$\mathcal{L}(f) = \int_0^{\infty} e^{-st} f(t) dt$$

as the Laplace transform. The initial conditions are assumed to be,

$$u_1(x_1, x_3, 0) = \frac{\partial}{\partial t} u_1(x_1, x_3, 0) = 0 \quad (1.5)$$

$$u_3(x_1, x_3, 0) = \frac{\partial}{\partial t} u_3(x_1, x_3, 0) = 0$$

Letting $\mathcal{F}[F(u_1)] = \bar{u}_1(k, x_3, s)$, $\mathcal{F}[F(u_3)] = \bar{u}_3(k, x_3, s)$, we have the following transformed equation:

$$C_{11}(-k^2) \bar{u}_1 + C_{55} \bar{u}_{1,33} + (C_{13} + C_{55}) (ik_1) \bar{u}_{3,3} = +s^2 \bar{u}_1 \quad (1.6)$$

$$C_{33} \bar{u}_{3,33} + C_{55}(-k^2) \bar{u}_3 + (C_{13} + C_{55}) (ik_1) \bar{u}_{1,3} = +s^2 \bar{u}_3$$

and at $x_3 = 0$, the transformed boundary conditions become

$$\bar{u}_{1,3} + ik_1 \bar{u}_3 = 0 \quad (1.7)$$

$$C_{33} \bar{u}_{3,3} + C_{13} ik_1 \bar{u}_1 = -p_0 \overline{f(k_1)g(s)}$$

Since we are expecting surface wave propagation, we seek the solution of (1.6), (1.7) in the forms:

$$\begin{bmatrix} \bar{u}_1 \\ \bar{u}_3 \end{bmatrix} = \begin{bmatrix} \phi_1 \\ \phi_2 \end{bmatrix} e^{-p(k,s)x_3} \quad (\text{real } (p) \geq 0) \quad (1.8)$$

Therefore, the equations for ϕ_1 , ϕ_2 are:

$$\begin{bmatrix} -s^2 - C_{11} k_1^2 + p^2 C_{55} & -ik_1 p (C_{13} + C_{55}) \\ -ik_1 p (C_{13} + C_{55}) & -s^2 - k_1^2 C_{55} + p^2 C_{33} \end{bmatrix} \begin{bmatrix} \phi_1 \\ \phi_2 \end{bmatrix} = 0 \quad (1.9)$$

or for a non-trivial solution,

$$\begin{aligned} \det = C_{33} C_{55} p^4 + [C_{33} (-s^2 - C_{11} k_1^2) + C_{55} (-s^2 - C_{55} k_1^2) + k_1^2 (C_{13} + C_{55})^2] p^2 \\ + (s^2 + C_{11} k_1^2) (s^2 + C_{55} k_1^2) = 0 \end{aligned} \quad (1.10)$$

We will choose the p 's with positive real parts to ensure the decay in x_3 direction of the surface wave. Let the solutions be $p = p_1, p_2$, therefore, we have

$$p = p_1 : \phi_1^{(1)} \equiv C_1(k_1, s), \quad \phi_2^{(1)} = - \frac{i[-s^2 - C_{11} k_1^2 + C_{55} p_1^2]}{k_1 p_1 (C_{13} + C_{55})} \quad (1.11)$$

$$p = p_2 : \phi_1^{(2)} \equiv C_2(k_1, s), \quad \phi_2^{(2)} = - \frac{i[-s^2 - C_{11} k_1^2 + C_{55} p_2^2]}{k_1 p_2 (C_{13} + C_{55})} \quad (1.11)$$

Therefore, the displacements have the forms:

$$\begin{bmatrix} \bar{u}_1 \\ \bar{u}_3 \end{bmatrix} = C_1(k_1, s) \begin{bmatrix} 1 \\ \psi_{31} \end{bmatrix} e^{-p_1 x_3} + C_2(k_1, s) \begin{bmatrix} 1 \\ \psi_{32} \end{bmatrix} e^{-p_2 x_3} \quad (1.12)$$

C_1 , C_2 are determined from the boundary conditions (1.7), or

$$\begin{bmatrix} -p_1 + ik_1 \psi_{31} & -p_2 + ik_1 \psi_{32} \\ -p_1 C_{33} \psi_{31} + ik_1 C_{13} & -p_2 C_{33} \psi_{32} + ik_1 C_{13} \end{bmatrix} \begin{bmatrix} C_1 \\ C_2 \end{bmatrix} = \begin{bmatrix} 0 \\ -p_0 \bar{fg} \end{bmatrix} \quad (1.13)$$

Here, the determinant, $\Delta(p_1, s)$, given by,

$$\begin{aligned} \Delta = & (ik_1 \psi_{31} - p_1) (ik_1 C_{13} - p_2 C_{33} \psi_{32}) \\ & - (ik_1 \psi_{32} - p_2) (ik_1 C_{13} - p_1 C_{33} \psi_{31}) \end{aligned} \quad (1.14)$$

must be non-zero to ensure a solution. ($\Delta=0$ gives the Rayleigh poles of the system, which correspond to a free surface). Therefore,

$$C_1 = \frac{1}{\Delta} [ik_1 \psi_{32} - p_2] \bar{fg} p_0 \quad (1.15)$$

$$C_2 = \frac{1}{\Delta} [p_1 - ik_1 \psi_{31}] \bar{fg} p_0$$

and the physical displacements $u_{11}^{(x_1, x_3, t)}$, $u_{31}^{(x_1, x_3, t)}$ are obtained by inverting their transforms.

From the stress-strain relations

$$\begin{aligned}
 t_{13} &= C_{55} (u_{1,3} + u_{3,1}), \quad t_{11} = C_{11} u_{1,1} + C_{13} u_{3,3}, \\
 t_{33} &= C_{33} u_{3,3} + C_{13} u_{1,1}
 \end{aligned} \tag{1.16}$$

we obtain the transforms of the stresses

$$\begin{aligned}
 \bar{t}_{13} &= C_{55} \{ (-p_1 + ik_1 \psi_{31}) C_1 e^{-p_1 x_3} \\
 &\quad + (-p_2 + ik_1 \psi_{32}) C_2 e^{-p_2 x_3} \} \\
 \bar{t}_{11} &= (C_{11} ik_1 - C_{13} p_1 \psi_{31}) C_1 e^{-p_1 x_3} \\
 &\quad + (C_{11} ik_1 - p_2 \psi_{32} C_{13}) C_2 e^{-p_2 x_3}
 \end{aligned} \tag{1.17}$$

$$\begin{aligned}
 \bar{t}_{33} &= (-p_1 \psi_{31} C_{33} + ik_1 C_{13}) C_1 e^{-p_1 x_3} \\
 &\quad + (-p_2 \psi_{32} C_{33} + C_{13} ik_1) C_2 e^{-p_2 x_3}
 \end{aligned}$$

and the physical stresses can be obtained by inversion.

The particular forcing function employed is

$$f(x_1) g(t) = [1 - \left(\frac{x_1}{a}\right)^2] \sin \frac{\pi t}{\tau_0} \quad 0 < t < \tau_0 \quad |x_1| \leq a$$
$$= [1 - \left(\frac{\lambda}{a}\right)^2 x_1^{*2}] \sin (\pi t^*/\tau_0^*) \quad (1.18)$$

where $\tau_0^* \equiv \lambda / \sqrt{C_{66}/\rho}$.

Here a is a length measuring the impact area, and τ_0 is the contact time [1]. The transform of this particular forcing function, in non-dimensional form becomes,

$$\overline{fg} = + \frac{4}{k^2 (a/\lambda)^2} \left[-\frac{a}{\lambda} \cos k_1 \left(\frac{a}{\lambda}\right) + \sin k_1 \left(\frac{a}{\lambda}\right) \right] \frac{\pi \tau_0^* (1 + e^{-s \tau_0^*})}{\pi^2 + \tau_0^{*2} s^2} \quad (1.19)$$

II. EDGE IMPACT OF PLATE WITH EDGE PROTECTION

To prevent failure of composite fan blades under impact forces, leading edge protective strips have been employed. In practice, these strips of stainless steel are wrapped around the leading edge. To model this device, we consider a beam bonded to the edge of an anisotropic plate (Figure 1). The effect of the beam will be to thwart the force of impact, thereby decreasing the normal stresses in the composite. However, we shall show that with such a reduction in normal stress, sizeable interface shear stresses can be induced.

With the introduction of a beam of thickness b on the edge of the composite plate, the Rayleigh wave behavior will depend on the ratio of the wavelength to thickness ratio of each Fourier component in the x_1 direction. Thus one should expect the Rayleigh wave speed to vary with b/a , the thickness to impact footprint ratio. In addition the Rayleigh wave will become distorted as it propagates.

To solve the edge strip problem the solution in the composite plate follows the same procedure as the no-strip case except for the boundary conditions on the edge. In place of the zero stress conditions on the edge we relate the edge stresses t_{33} , t_{13} to the motion of the beam strip. If one considers a small element of the beam-strip along the x_1 direction, the momentum balance equations in the x_1 , x_3 directions become, (for a plate of unit thickness)

$$\rho b \frac{\partial^2 U}{\partial t^2} = E b \frac{\partial^2 U}{\partial x_1^2} + t_{13} \quad (2.1)$$

$$\frac{\rho b}{\partial t^2} \frac{\partial^2 W}{\partial x_1^4} = - EI \frac{\partial^4 W}{\partial x_1^4} + I_p b \frac{\partial^4 W}{\partial x_1^2 \partial t^2} + \frac{b}{2} \frac{\partial t_{13}}{\partial x_1} + t_{33} + p_0^f g \quad (2.2)$$

In these equations U, W are the x_1, x_3 displacements of the beam element at the half thickness, and t_{33}, t_{13} are the interface stresses.

We choose the compatibility conditions between the beam and plate displacements

$$W = u_3, \text{ on } x_3 = 0. \quad (2.3)$$

$$U = u_1 + \frac{b}{2} \frac{\partial u_3}{\partial x_1}, \text{ on } x_3 = 0 \quad (2.4)$$

In the above equations b is the depth of the strip, E, I, I_p are respectively the Young's modulus, moment of inertia and rotary inertia. Also $p f(t) g(x_1)$ is the edge loading now applied to the outer protective strip surface.

The equations for the plate remain as in the free edge case and a solution is obtained by taking a Laplace transform on time and a Fourier transform on the space variable x_1 . With nondimensionalization the solution in the plate is assumed in the form of (1.12). The transform of the plate displacements are

$$\begin{bmatrix} \bar{u}_1 \\ \bar{u}_3 \end{bmatrix} = C_1 \begin{bmatrix} 1 \\ \psi_{31} \end{bmatrix} e^{-p_1 x_3} + C_2 \begin{bmatrix} 1 \\ \psi_{32} \end{bmatrix} e^{-p_2 x_3} \quad (2.5)$$

where p_1, p_2 are defined in (1.10) and ψ_{31}, ψ_{32} are given in (1.11). C_1, C_2 are determined from the edge boundary conditions. However, in place of the free edge conditions (1.2) we use the equations of motion for the strip (2.1),

(2.2). C_1, C_2 are then solutions to the algebraic equations

$$\begin{bmatrix} G_1 & H_1 \\ G & H \end{bmatrix} \begin{bmatrix} C_1 \\ C_2 \end{bmatrix} = \begin{bmatrix} 0 \\ -p_0^* \bar{fg} \end{bmatrix} \quad (2.6)$$

where

$$G_1 = -k^2 Ew + p_1 C_{55} - \rho ws^2 - \psi_{31} (ik^2 w^2 E/2 + ikC_{55} + \rho w^2 s^2 ik/2)$$

$$H_1 = -k^2 Ew + p_2 C_{55} - \rho ws^2 - \psi_{32} (ik^3 w^2 E/2 + ikC_{55} + \rho w^2 s^2 ik/2)$$

$$\begin{aligned} G = & -ikC_{13} + ikwp_1 C_{55}/2 + \psi_{31} (p_1 C_{33} + Ew^2 k^4/12 + wk^2 C_{55}/2 \\ & + k^2 s^2 \rho w^3/2 + \rho ws^2) \end{aligned}$$

$$\begin{aligned} H = & -ikC_{13} + ikwp_2 C_{55}/2 + \psi_{32} (p_2 C_{33} + Ew^2 k^4/12 + wk^2 C_{55}/2 \\ & + k^2 s^2 \rho w^3/2 + \rho ws^2) \end{aligned} \quad (2.7)$$

where $w = b/\ell$, ρ , E , are nondimensionalized quantities and $p_1, p_2, \psi_{31}, \psi_{32}$ are defined in (1.11).

III. NUMERICAL INVERSION

The inversions are accomplished by the Fast Fourier Transform (FFT) techniques [2], which consists of a transformation from Laplace to Fourier transforms, and a two-dimensional numerical inversion using the usual FFT algorithm. Notice the Laplace inversion formula

$$f(t) = \frac{1}{2\pi i} \int_{\Gamma}^{C+i\infty} f(s) e^{st} ds$$

Set $s = C + i\alpha$

$$f(t) = \frac{1}{2\pi} \int_{-\infty}^{\infty} f(C+i\alpha) e^{Ct} e^{i\alpha t} d\alpha \quad (3.1)$$

where C and α are both real, and C is greater than the largest real part of all singularities of $f(s)$. Numerically, the double Fourier transform (or inversion) has the following form [1]:

$$f(x, t) \approx \frac{K_x K_t}{\pi^2 NM} e^{-i[K_x(1-\frac{1}{N})x + K_t(1-\frac{1}{M})t]} \sum_{I=1}^N \sum_{J=1}^M \bar{f}(I, J) e^{2\pi i [\frac{(I-1)x}{N} + \frac{(J-1)}{M} t]} \quad (3.2)$$

where N, M are the number of points in x and t direction respectively, and K_x, K_t are the corresponding half-frequency range.

For the present problem, the determination of C is through the following considerations:

The form of inversion integrals are, in general,

$$I = \frac{1}{2\pi i} \int_{C-i\infty}^{C+i\infty} \frac{F(k_1, s)}{\Delta(k_1, s)} e^{-px_3} e^{st} ds \quad p = p(k_1, s), \operatorname{Re}(p) \geq 0 \quad (3.3)$$

and Δ is given by (1.14). It is easy to see the singularities of the integral of (2.3) are:

a) Poles at $\Delta = 0$,

$$\Delta = (p_2 - p_1) ik_1 (C_{13} - \psi_{31} \psi_{32} C_{33}) + (\psi_{32} - \psi_{31}) (k_1^2 C_{13} + p_1 p_2 C_{33}) = 0 \quad (3.4)$$

implies

$$(p_2 - p_1) [C_{13} k_1^2 p_1 p_2 (C_{13} + C_{55})^2 + C_{33} (C_{55} p_1^2 - s^2 - C_{11} k_1^2) (C_{55} p_2^2 - s^2 - C_{11} k_1^2)] - (C_{13} + C_{55}) [p_1 (C_{55} p_2^2 - s^2 - C_{11} k_1^2) - p_2 (C_{55} p_1^2 - s^2 - C_{11} k_1^2)] (k_1^2 C_{13} + p_1 p_2 C_{33}) = 0 \quad (3.5)$$

Interpretation of this condition is best understood
for the particular case of an isotropic material, i.e. for

$$C_{11} = \lambda + 2\mu = C_{33}, \quad C_{13} = \lambda, \quad C_{55} = \mu,$$

$$\text{choose } C_{66} = C_{55} = \mu$$

It is easy to see that from (1.10), (1.11)

$$\det = [\mu p_1^2 - (\mu k_1^2 + \rho s^2)] \{ (2\mu + \lambda) p_1^2 - [(\lambda + 2\mu) k_1^2 + \rho s^2] \}$$

$$p_1^2 = (\mu k_1^2 + \rho s^2)/\mu, \quad p_2^2 = [(\lambda + 2\mu) k_1^2 + \rho s^2]/(\lambda + 2\mu)$$

$$\psi_{31} = ik_1/p_1, \quad \psi_{32} = -p_2/ik_1,$$

Here $[\mu/\rho]^{1/2} \equiv v_s$, is the shear wave speed and $[(\lambda + 2\mu)/\rho]^{1/2} v_p$, is the longitudinal or pressure wave speed for isotropic materials.

Thus for the isotropic case that, $\Delta = 0$ implies

$$4\mu p_2 + (p_1 + \frac{k^2}{p_1}) [\lambda + \frac{p_2^2}{k^2} (\lambda + 2\mu)] = 0 \quad (3.6)$$

where p_1, p_2 are defined above. This is the equation for the Rayleigh wave speed $v_R \equiv (is/k)^{1/2}$ which is found as a real root of (3.6) (see e.g. [3]).

For the case $\lambda = \mu$ (Poissons ratio = 0.25), $v_R = 0.919 v_s$.

For the anisotropic case a computational scheme to calculate the zeroes of (3.5) has been written, (Figure 2).

b) Branch points: The branch points of the integrand in (3.3) are the same as those of the functions $p_1(k, s), p_2(k, s)$, they are:

i) $p_1 = 0$, or $p_2 = 0$ which implies $(C_{11} k^2 + \rho s^2) (C_{55} k^2 + \rho s^2) = 0$
i.e., $k/s = \pm i\sqrt{\rho/C_{55}}$, $\pm i\sqrt{\rho/C_{11}}$ pure imaginary.

These correspond to longitudinal and shear wave speeds for an isotropic material

ii) $p_{1,2} = \pm \sqrt{-B \pm \sqrt{B^2 - 4AC}} / 2A \quad (3.7)$

with $A = C_{33} C_{55} > 0$

$$B = -\rho s^2 (C_{33} + C_{55}) + k^2 [(C_{13} + C_{55})^2 - C_{11} C_{33} - C_{55}^2]$$

$$C = (C_{11} k^2 + \rho s^2) (C_{55} k^2 + \rho s^2)$$

These branch points are those values of s/k which render $B - 4AC = 0$, and are branch points of second order.^[4] The distribution of these points is shown in Figure 3. It has been shown [5] that the contribution of these branch points to the value of the integrals (3.3) is important only when one considers the multi-reflected and refracted waves in layered media, or when the position of interest is very close to the impact origin. In this study we were more concerned with how the energy is propagated away from the impact point, which is mainly associated with surface waves, thus we ignored the contribution of these branch points.^[5]

The contour of integration for the Laplace inversion is as shown in Figure 3. Notice the branch cuts are extended to negative infinity, in accordance with the requirement that $C > \max$ real part of the singularities. The requirement that $\text{real}(p) \geq 0$ also determines the correct sheet of the Riemann surfaces. Numerically, since the branch points are located at $s/k = \text{constant}$, as k gets large C should be large, and the factor e^{ct} in the Laplace inversion expression will rise sharply to an unmanageable size. Since, in the last paragraph, we have noticed the contribution of the branch points is unimportant, a path Γ_2 is chosen to replace Γ_1 by the Cauchy's integral theorem. Notice the advantage of integration along Γ_2 is that C_0 is a positive constant independent of k . The determination of optimal C_0 is discussed in [2]. Here, in order to minimize the aliasing and round off errors in numerical computations simultaneously, we choose

$$C_0 = \frac{2}{3M\lambda_t} \ln (\hat{g}/\hat{r}) \quad (3.9)$$

where $\hat{g} = p_0/C_{66}$, $\hat{r} = 10^{-6} \times \frac{1}{\lambda_t}$. λ_t is a small time interval, less than the impact contact time. Further details are given in Appendix A.

IV. RESULTS

A computer program has been written to calculate the stresses in a plate with an elastic beam on one edge under a transient impact load distribution along the edge. A program description, flow charts, input data formats, and sample printout of the program are contained in the appendices to this report. In this section we will summarize some of the results obtained from this computer program. These results were calculated for an anisotropic plate with effective elastic constants of 55% graphite fiber/epoxy matrix composite obtained from Reference 7 and summarized in the Table.

No-strip case:

The Rayleigh wave can be seen in the stress t_{11} on the edge as shown in Figures 4, 5 for a graphite fiber-epoxy composite for layup angles $0, \pm 15^\circ$. After the initial contact time, the stress is observed to propagate with little change at a speed near the calculated Rayleigh speed (Figure 2). This wave can be observed in the computed output in the space-time $(x_1, -t)$ plane Figure 7, as a band of non-zero values along a diagonal from the upper left to the lower right corner of the $x_1, -t$ plane. Caution is urged in using this program since spurious waves can enter the calculations due to the periodic nature of the finite numerical Fourier Transform. These spurious waves are data bands which lie along diagonals from upper right to lower left. In other words, only disturbances emanating from the impact source in the upper left corner of the $x_1 - t$ plane of Figure 7 should be valid. A computer map of the space time history of the edge impact stress is shown in Figure 6. A contact time of 35 μ sec and contact length 2 cm was used in these calculations.

As is characteristic of surface wave effects, the stresses due to impulsive loading on the edge decrease with distance from the edge. This is shown in Figure 8 for two different layup angles. The normal stress t_{33} appears to decrease to about 1/4 of its value on the surface at a depth equal to one half of the loading length a . The rate of decay from the edge depends on the layup angle. Another characteristic of edge impact is the development of tension in the normal stress t_{33} under the impact point. This is shown in Figure 9. Thus while the compression part decreases with distance from the edge a tension tail develops in the wave.

The effect of layup angle on the impact stresses can be seen in Figures 10, 11. The stress t_{11} at the edge is larger than the impact pressure and decreases as the layup angle goes from 0° to $\pm 45^\circ$ (Figure 10).

Below the surface or edge, the peak normal stress t_{33} at $x_1 = 0$ is a minimum for layup angles near $\pm 30^\circ$, while the shear stress t_{13} increases as the fiber angle goes from 0° to $\pm 45^\circ$ (Figure 10).

An unexpected result is the shift of the maximum normal stress t_{33} to points off the impact axis $x_1 = 0$ for layup angles greater than about ± 30 . A pronounced peak in t_{33} versus x_1 , beyond the impact pressure foot print, can be seen in Figure 11 for $\pm 45^\circ$ layup angle.

Impact protection strip case:

The effect of bonding an edge impact protection strip to the half plane is shown in Figures 12-16. In Figures 12, 13, the increase in the thickness of a steel strip produces a decrease in the interface stresses

t_{11} , t_{33} but creates an interface shear stress at the strip-composite interface. This shear stress reaches a maximum for strip thickness less than the impact footprint length and decreases for greater strip thicknesses. Thus, if the strip is too thin, debonding can occur under impact due to induced interface shear.

In Figure 14 one can see that increasing the strip thickness decreases the peak normal stress t_{33} and redistributes the load over a longer length under the strip. However, while the peak compression stress is decreased by the strip, tension is created which could also produce debonding of the strip from the composite.

For the no-strip case a Rayleigh wave was seen to propagate along the edge relatively unperturbed (Figures 4, 5). With the strip present, (Fig.15) this wave becomes distorted as time increases. In fact, the beam-strip boundary conditions introduce dispersion in the edge waves which make the Rayleigh edge wave velocity dependent in the effective wave length of the disturbance.

Finally in Figure 16 shear stress distributions along the strip-composite interface are shown for a thickness near the shear peak ($b/a = 0.25$) and another for $b/a = 2.0$. In the latter case the shear is distributed over a larger length resulting in a lower peak stress. Also the strip delays the time of maximum shear from $1/2$ to $3/4 T_0$

Summary of Results

An analytical-numerical method has been developed to solve the response of a composite plate with a bonded edge strip to in-plane impact type forces on the edge. Results of computer simulations reveal the following:

- 1) Rayleigh edge waves can propagate away from the impact site with tension and compression up to values of the impact pressure, depending on layup angle.
- 2) Normal to the edge, the initial peak compression pulse decreases as it propagates into the plate but a tension tail develops as it propagates away from the impact site.
- 3) The edge stress t_{11} under impact is decreased as the fiber layup angle goes from 0° to $\pm 45^\circ$.
- 4) Protection strips of thickness less than half the impact length can develop large interface shear under impact.
- 5) The normal and edge stresses t_{33} , t_{11} at the edge can be decreased significantly by protection strips of thickness greater than the half impact length.

REFERENCES

- [1] Moon, F. C., Theoretical Analysis of Impact in Composite Plates, NASA CR-121110, 1973.
- [2] Cooley, J. W., Lewis, P. A. W., and Welch, P. D., The Fast Fourier Transform Algorithm, J. Sound Vibration, 1970, v. 12 (3), pp 315-337.
- [3] Fung, Y. C., Foundations of Solid Mechanics, 1968, Prentice Hall, pp 180.
- [4] Kraut, E. A., Advances in the Theory of Anisotropic Elastic Wave Propagation, Review of Geophysics, 1,3, 1963, pp 401-448.
- [5] Ewing, W. M., Jardetzky, W. S. and Press, F., Elastic Waves in Layered Media, 1957, McGraw-Hill, N.Y., pp. 142.
- [6] Buchwald, V. T., Rayleigh Waves in Transversely Isotropic Media, Quart. J. Appl. Mech. & Math., v. 16 (3), 1961, pp. 293-317.
- [7] Chamis, C. C., Computer Code for the Analysis of Multilayered Fiber Composites, Users Manual NASA TN D-7013, 1971.
- [8] Premont, E. J., Stubenrauch, K. R., Impact Resistance of Composite Fan Blades, Pratt and Whitney Aircraft report PWA 4763, prepared for NASA-Lewis Research Center, NASA CR-134515, May 1973.
- [9] Stoneley, R., "The propagation of surface waves in anisotropic media" from Partial Differential Equations and Continuum Mechanics, Ed. R. E. Langer, Univ. of Wisconsin Press, Madison 1961 pp.81-93

TABLE I. - STRESS-STRAIN COEFFICIENTS FOR 55 PERCENT GRAPHITE
FIBER-EPOXY MATRIX COMPOSITE

[All constants to be multiplied by 10^6 psi; data obtained from ref. 7.]

0° Layup						$\pm 15^\circ$ Layup					
27.95	0.3957	0.3957	0	0	0	24.56	0.4000	1.986	0	0	0
1.170	0.4601	0	0	0	0	1.170	0.4558	0	0	0	0
1.170	0	0	0	0	0	1.374	0	0	0	0	0
0.3552	0	0	0	0	0	0.3552	0	0	0	0	0
			0.7197	0	0.3552			2.310	0		0.3552
$\pm 30^\circ$ Layup						$\pm 45^\circ$ Layup					
16.48	0.4118	5.167	0	0	0	8.197	0.4279	6.758	0	0	0
1.170	0.4400	0	0	0	0	1.170	0.4279	0	0	0	0
3.093	0	0	0	0	0	8.179	0	0	0	0	0
0.3552	0	0	0	0	0	0.3552	0	0	0	0	0
	5.491	0	0	0	0.3552			7.082	0		0.3552

APPENDIX A

The Determination of Parameter C_0

Consider the Laplace inversion of a function $g(t)$ as

$$g(t) = \frac{1}{2\pi i} \int_{C_0 - i\infty}^{C_0 + i\infty} \bar{g}(s) e^{st} ds \quad (A.1)$$

and let $s = C_0 + i\omega$, C_0 and ω are real. We can change (A.1) into the Fourier inversion formula

$$g(t) = \frac{1}{2\pi} e^{C_0 t} \int_{-\infty}^{\infty} \bar{g}(C_0 + i\omega) e^{i\omega t} d\omega \equiv e^{C_0 t} x(t) \quad (A.2)$$

which is then inverted by the Fast Fourier Transform technique. In the FFT scheme, a continuous function $\bar{g}(C_0 + i\omega)$ is discretized and the infinite interval of integration is truncated. The error due to truncation depends on each problem but doesn't depend on C_0 , thus in the determination of C_0 , we will assume the truncation error is negligible. It is shown [2] that the discretizing of the transform in one domain will cause aliasing error in the other domain, e.g. sampling \bar{g} at N points in a frequency interval, $0 < \omega < \Omega$, will produce a transformed function $x_p(t)$ which is periodic and which differs substantially from $x(t)$ for large enough t . For even $x(t)$ this difference can be shown [2] to be given by,

$$x_p(t) \approx x(t) + x(t-T)$$

for $0 < t < T/2$ where $T = N/\Omega$.

It has been shown [2] also that the aliasing error is approximated by $E_a(t) = e^{-C_o(T-2t)} g(T-t)$ for the Laplace inversion (A.2).

Notice the aliasing error is a decreasing function of C_o .

The other source of error is of course the round off error in computation. Since we multiply the resulting $x(t)$ by $e^{C_o t}$ to get $g(t)$, the rounding error is of the form

$$Er(t) = e^{C_o T} r(t).$$

The error bounds are then

$$\left. \begin{aligned} \varepsilon_1 &= \left| \max E_a(t) \right| = e^{-C_o(T-2\tau)} \max |g(T-t)| \\ \varepsilon_2 &= \left| \max Er(t) \right| = e^{C_o \tau} \max |r(t)| \end{aligned} \right\} \quad 0 \leq t \leq \tau$$

Equating ε_1 and ε_2 , the optimal C_o is then

$$C_o = \frac{\ln(\max g(T-t)/\max r(t))}{T-\tau}$$

Choosing $\tau = T/4$, therefore

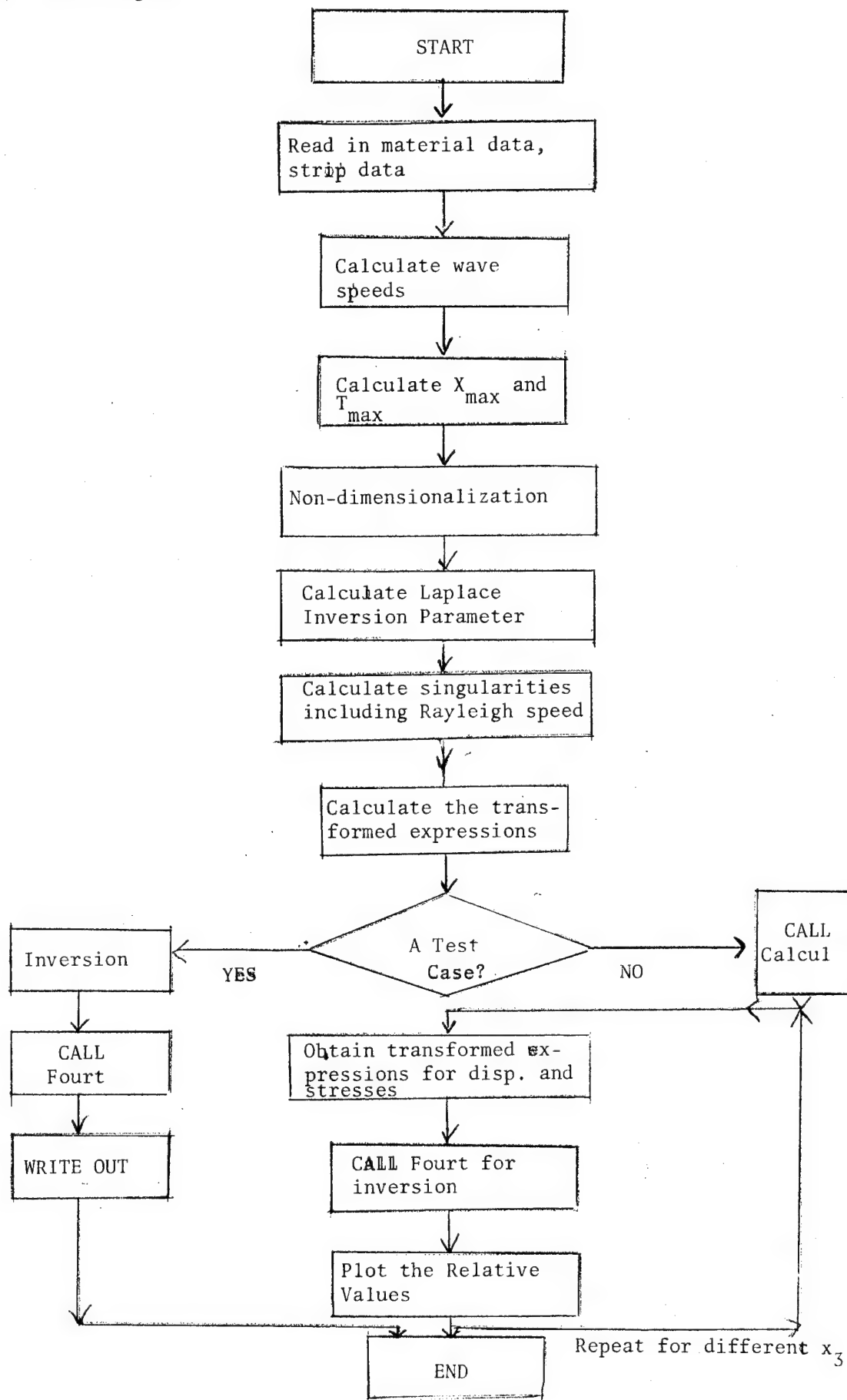
$$C_o = \frac{4}{3T} \ln(\hat{g}/\hat{r}), \quad \hat{g} \equiv \max g(T-t), \quad \hat{r} \equiv \max r(t)$$

Notice, empirically, $\hat{r} \approx 2 \frac{N}{T} 10^{-6}$ on single precision IBM 360 systems.

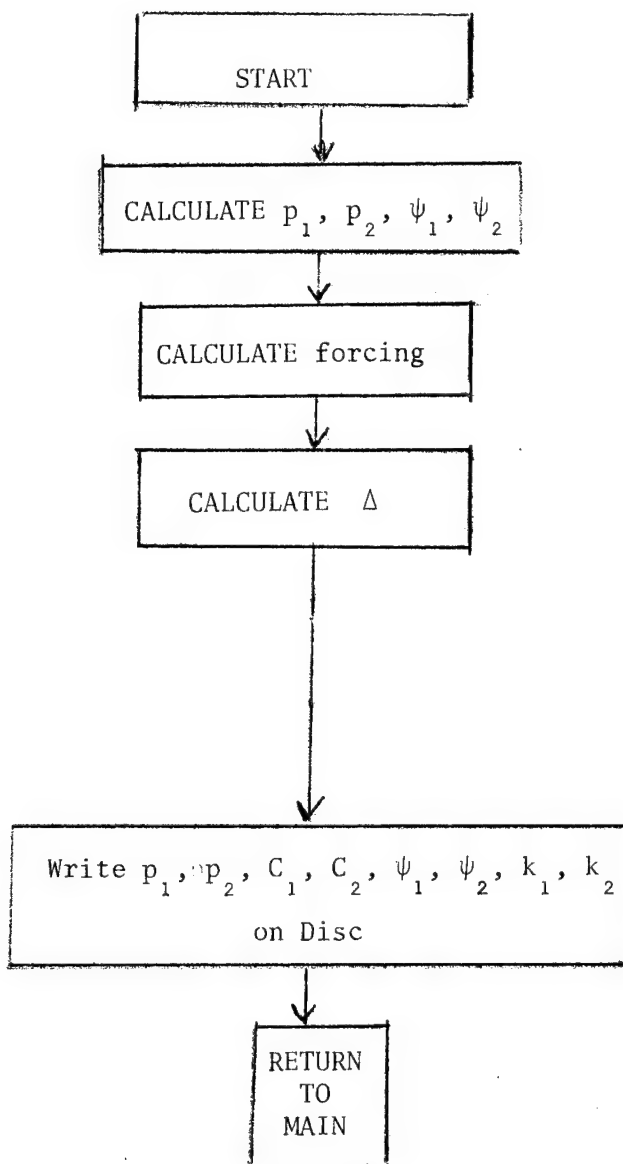
APPENDIX B

A FLOW CHART OF THE PROGRAM

1. Main Program



3. Subroutine calcul



APPENDIX C

NOTES ON COMPUTER PROGRAM

The choice of scales is very essential to the success of the present computational method. It is noticed that the accuracy depends on the number of points employed and the range of frequency spectra covered. Considering limitations of both computer storage and time, a time-space grid of 32×64 points was chosen for $t > 0$, $x_1 > 0$. Thus, the non-dimensionalization of all equations and quantities are both necessary and important to the obtaining of meaningful data from the limited grid size.

The numerical inaccuracies introduced have several origins:

1. Theoretically, error has been introduced by the neglecting of the outer branch points contributions. It has been shown, for isotropic cases, the contributions of these branch points behaved like r^{-2} at large distance from a delta function loading at the origin $r = 0$. Compared with the $r^{-\frac{1}{2}}$ decreases of the contribution of the residue. Thus, for small r , or near the origin, the errors might be significant. An asymptotic form of the behavior of small r has been deduced for a simple delta loading at origin on an isotropic half-space []. It is shown the error thus introduced is of the order of 5% maximum response in stress.
2. The aliasing error introduced through the periodizing of the functions.
3. The round-off error in Laplace inversion along with aliasing error. have been discussed in the determination of C_0 (Appendix A). It is

found that error 3 is more serious of the two. Hence in calculations the maximum non-dimensionalized time should be restricted to below 6 or 8 for reasonably good results.

4. Errors due to reflections at the boundary. Since the space grid is finite, it has been observed that whenever a wave hit the boundary of chosen space, a sizable numerical error will start propagating in, as if the wave were reflected from the boundary. The basic reason is due to the periodization of the space (x_1) domain. In computation, this error should be avoided. To correctly determine the extent of the space (x_1) domain, a priori recognition of significant wave speed (at which most of the energy travels) is important. Usually an estimation will be sufficient. Then the proper nondimensionalizing constants can be chosen.

APPENDIX D
PROGRAM INPUT AND OUTPUT

A. Method:

FFT alogarithm for numerical inversion

B. Input Data Cards:

Card 1. NTEST, NSTRIP, NP (315)

NTEST = 1 A test program for FFT (2-D) (beam).

0 The present program

NSTRIP = 1 With strip

0 No strip

NP = 1 Calculate: u_1 only

2 u_1, u_3

3 u_1, u_3, t_{33}

4 u_1, u_3, t_{33}, t_{11}

5 $u_1, u_3, t_{33}, t_{11}, t_{13}$

Card 2. CC(I) I = 1,9, RHO, ANGLE (8E10,4)

CC(I=1,9) Material constants of composite, in the order

$C_{11}, C_{22}, C_{33}, C_{44}, C_{55}, C_{66}, C_{12}, C_{13}, C_{23}$. (psi)

RHO Density of composite (g/cm³)

ANGLE (degrees) lay-up angle

Card 3. VEL, DM, E1, ANU, DEN (8E10.4)

VEL - Velocity of incoming particle m/sec

DM - Diameter of impacting object cm

E1 - Youngs Modulus of impacting object (psi)

ANU - Poissons ratio of impacting object

DEN - Density of impacting object (gm/cc)

Card 4. NSTRES, NK3, DX3 (215, F10,3)

NSTRES = 1

NK3: Number of steps in x_3 direction

DX3: $\Delta x_3 / \ell$, step size in x_3 direction

Photo elastic fringe order computer map in the x-t plane.

Card 5. RO, W, ES (3E10,4)

RO: density of strip beam (g/cm³)

W: depth of strip beam (cm)

ES: Young's modulus of strip beam (psi)

C. Output:

1. Test problem: Appendix III

2. Values of displacements 1 : u_1

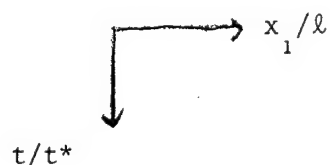
2 : u_3

(stress) 3 : σ_{33}

4 : σ_{13}

5 : σ_{11}

3. Relative magnitude computer maps of displacements and stresses.



FORTRAN IV G LEVEL 21

MAIN

DATE = 74186

11/28/2

* This program has two extra cards to override the Hertz contact time and contact length calculation. Remove cards #51, 52.

C W, THICKNESS TO WIDTH RATIO OF BEAM
 C ES, YOUNG'S MODULUS FOR BEAM
 C WL--FOURIER WAVELENGTH (CM) OF THE ORDER OF A0 OR LESS
 C WT--FOURIER WAVE PERIOD (SEC) OF THE ORDER OF T0 OR LESS
 C CHOICE OF WL,WT DETERMINES DX,DT--DX=WL/2,DT=WT/2
 C FG, TRANSFORM OF NORMALIZED FORCING FUNCTION F(X1)*G(T)
 C THIS IS PROVIDED IN PROGRAM BUT CAN BE CHANGED BY THE USER
 C
 C OUTPUT DATA
 C T0,TC CONTACT TIME (SEC,1.E-6 SEC) (FROM HERTZ THEORY)
 C A0,A, HALF THE IMPACT CONTACT LENGTH ,CM
 C FO, MAX IMPACT FORCE FROM HERTZ THEORY , NEWTONS
 C E, WAVE SPEED IN PLATE SQRT(C66/RHO)
 C OR WAVE SPEED IN BEAM STRIP, SQRT(E1/DEN) UNITS CM/SEC
 C CL=SQRT(C11/RHO) LONGITUDINAL WAVE SPEED ALONG EDGE IN PLATE
 C CS=SQRT(C55/RHO), SHEAR SPEED ALONG EDGE OF PLATE,CM/SEC
 C CR, RAYLEIGH WAVE SPEED ALONG FREE EDGE OF PLATE
 C
 C DX,DT SPACE TIME INCREMENTS IN X1-T SPACE UNITS--CM AND SEC
 C DATA(I,J) ,NORMALIZED TRANSFORM OF ONE OF DISPL. OR STRESSES
 C --BEFORE CALL FOURT,AFTER CALL FOURT DATA IS A 2 DIM MATRIX OF
 C DISPL. OR STRESSES IN X1-T SPACE,DEPENDING ON VALUE OF K
 C IN THE LOOP 'DO 4 K=1,NP'
 C U1,U3,NORMALIZED DISPL. IN PLANE OF PLATE (E.G. U1/A0)
 C T33,T11,T13, NORM. STRESSES (E.G. T33/C66)
 C --NOTE-- T33 ON X3=0 SHOULD REPRODUCE THE FORCING FUNCTION
 C WHEN THERE IS NO STRIP
 C --NOTE-- AS A CHECK T13=0 ON X3=0 WHEN THERE IS NO STRIP
 C THE FRINGE ORDER MAP PLOTS THE DIFF IN PRINCIPAL STRESSES AND
 C MAY BE USED TO COMPARE WITH PHOTOELASTIC EXPERIMENTS OR TO
 C LOOK FOR POINTS OF MAX IN PLANE SHEAR STRESSES
 C *****
 C THIS PROGRAM HAS BEEN WRITTEN BY F.MOON AND C-K KANG UNDER
 C A GRANT TO PRINCETON UNIVERSITY FROM THE NASA LEWIS RESEARCH
 C LAB.
 C *****
 C --NOTE TO THE USER-- IN THE OUTPUT MAPS OF STRESSES OR DISPL.,
 C YOU WILL NOTICE BANDS OF SIMILAR NUMBERS RUNNING FROM THE
 C UPPER LEFT CORNER TO THE LOWER RIGHTCORNER -- THESE ARE WAVES
 C WHICH EMINATE FROM THE IMPACT POINT--HOWEVER- WAVES RUNNING
 C FROM RIGHT UPPER TO LEFT LOWER CORNER ARE SPURIOUS DUE TO THE
 C DISCRETENESS OF THE NUMERICAL FOURIER INVERSION PROGRAM
 C --ALSO DATA FOR TIMES NEAR TMAX AT THE BOTTOM OF THE MAPS ARE
 C USUALLY SPURIOUS AND SHOULD NOT BE USED

```

0001 COMMON /MMC/ D,DK1
0002 COMMON /MC/DK2,FG1,T0,C11,C13,C33,C55,RHO,RO,W,ES,NSTRIP,A0
0003 DIMENSION DATA(128,32),MM(40),CC(9)
0004 DIMENSION NN(2)
0005 DIMENSION RDATA(40)
0006 DIMENSION CIDATA(40)
0007 DIMENSION FRNGE(64,32)
0008 DIMENSION T11(64,32),T33(64,32),T13(64,32)
0009 COMPLEX DATA,S
0010 COMPLEX P1,P2,S1,S2,C1,C2,B,C,D,SI
0011 COMPLEX DK2,FG,SLAP,DK1
  
```

FORTRAN IV G LEVEL 21

MAIN

DATE = 74186

11/28/2

```
0012      CCMPLEX*16 BS
0013      NN(1)=128
0014      NN(2)=32
0015      C*** READ IN AND WRITE OUT DATA AND PARAMETERS
0016      C*** RHO,A0,T0 MUST BE IN C.G.S. UNITS, P0 MUST BE CONSISTENT WITH CC
0017      CALL INDUMP
0018      READ (5,102) NTEST,NSTRIP,NP
0019      READ (5,100) CC,RHO,ANGLE
0020      WRITE(6,490) CC
0021      WRITE(6,491) RHO,ANGLE
0022      READ(5,100) VEL,DM,E1,ANU,DEN
0023      P0=CC(6)
0024      C11= CC(1)-CC(7)**2/CC(2)
0025      C33= CC(3)-CC(9)**2/CC(2)
0026      C13= CC(8)-CC(7)*CC(9)/CC(2)
0027      C55= CC(5)
0028      PI= 3.14159265
0029      RHO= RHO/6.895*1.E-4
0030      READ (5,101) NSTRES,NK3,DX3
0031      WRITE (6,504) NSTRES,NK3,DX3
0032      SI= CMPLX(0.,1.)
0033      C***** CALCULATE THE IMPACT CONTACT TIME ,RADIUS,AND PRESSURE
0034      C***** BASED ON HERTZ CONTACT THEORY
0035      R=DM/2.0
0036      R=R*1.E-2
0037      E1=E1*6895.0
0038      E2=CC(2)*6895.0
0039      DEN=DEN*1.0E3
0040      AMASS=4./3.*PI*R**3*DEN
0041      AK2=4./3.*SQRT(R)*E1/((1.0-ANU*ANU)+E1/E2)
0042      ALF=5./4.*AMASS*VEL*VEL/AK2
0043      ALF=(ALF)**0.4
0044      TC=2.943*ALF/VEL
0045      F0=1.14*AMASS*VEL*VEL/ALF
0046      A=SQRT(ALF*R)
0047      A=1.0E2*A
0048      TC=TC*1.0E6
0049      WRITE(6,710) VEL,TC,A,F0
0050      C***** CALCULATE THE NON-DIMENSIONAL PARAMETERS
0051      C*** UNIT DISTANCE --CM.
0052      A0=A
0053      T0=TC*1.E-6
0054      C     TEST CASE T0== 35E-6, A0=1 CM
0055      A0=1.0
0056      T0=35.E-6
0057      AL=A0
0058      C*** UNIT TIME--SEC.
0059      TE=AL/E
0060      C*** SMALLEST WAVELENGTHS
0061      WL=AL/1.5
0062      WT=TC/10.0
```

FORTRAN IV G LEVEL 21

MAIN

DATE = 74186

11/28/21

```

C*** DIMENSIONS OF TRANSFORM SPACE
0057    XK=2.0*PI*AL/WL
0058    TK=2.0*PI*TE/WT
C*** NCNDIMENSIONALIZE CONSTANTS
0059    A0=A0/AL
0060    T0=T0/TE
0061    DT=WT/2.0
0062    DX=WL/2.0
0063    WRITE(6,621) WT,WL,TK,XK
C*****CALCULATE RAYLEIGH WAVE SPEED
C
0064    X1=0.0
0065    X2=C55
0066    N=0
0067    DO 90 I=1,100
0068    N=N+1
0069    X=(X1+X2)/2.0
0070    D1=(C55-X)/(C11-X)
0071    D1=SQRT(D1)
0072    D2=(C13)**2-C33*(C11-X)
0073    D3=C55*C33
0074    D3=SQRT(D3)
0075    F=D1*D2/D3
0076    F=X+F
0077    IF(F) 81,82,83
0078    81 X1=X
0079    GO TO 92
0080    82 GO TO 91
0081    83 X2=X
0082    92 CONTINUE
0083    F1=F/C55
0084    DIFF=ABS(F1)-1.0E-4
0085    IF(DIFF) 91,91,90
0086    90 CONTINUE
0087    91 CONTINUE
0088    WRITE(6,701) C11,C33,C55,C13
0089    701 FORMAT(//,10X,6H C11 =,E12.4,6H C33 =,E12.4,6H C55 =,E12.4,
16H C13 =,E12.4,/)
0090    CL=C11/RHO
0091    CL=SQRT(CL)
0092    CS=C55/RHO
0093    CS=SQRT(CS)
0094    CR=X/RHO
0095    CR=SCRT(CR)
0096    RDS=CR/CS
0097    WRITE(6,702) CL,CS,CR,RDS,N
0098    702 FORMAT(//,10X,12H LONG SPEED =,E12.4,13H SHEAR SPEED =,E12.4
1 //,10X,16H RAYLEIGH SPEED =,E12.4,8H CR/CS =,F10.5,5X,15)
C*****CONSTANTS FOR STRIP CASE
C*** CONSTANTS FOR STRIP CASE
0099    READ (5,100) RO,W,ES
0100    WRITE(6,521) RO,W,ES
0101    RO= RO/6.895*1.E-4
0102    IF (RO) 51,51,50
0103    50 CONTINUE
0104    E= SQRT(ES/RO)

```

FORTRAN IV G LEVEL 21

MAIN

DATE = 74186

11/28/2

```
0105      WRITE (6,510) E
0106      51 CONTINUE
0107      RO= RO/RE
0108      ES= ES/EE
0109      W= W/A0/AL
0110      ****
0111      205 CONTINUE
0112      C11= C11/EE
0113      C13= C13/EE
0114      C33= C33/EE
0115      C55= C55/EE
0116      P0= P0/EE
0117      RHO= RHO/RE
0118      FG1= P0*T0
0119      206 CONTINUE
0120      N= NN(1)
0121      C*** CALCULATE THE LAPLACE INVERSION PARAMETER
0122      WT= WT/TE
0123      RH= P0*WT*1.E6
0124      CH= 2./3./M/WT*ALOG(RH)
0125      CLAP= CH
0126      C*** CALCULATE THE SECOND ORDER BRANCH POINTS
0127      A= RHO*(C33-C55)**2*RHO
0128      E= -2.*RHO*((C33+C55)*(C13*C13+2.*C13*C55-C11*C33)+2.*C33*C55
0129      1*(C11+C55))
0130      F= (C13*C13+2.*C13*C55-C11*C33)**2-4.*C11*C33*C55*C55
0131      BS= 1.D0*E*E-1.D0*4.*A*F
0132      D= CDSQRT(BS)
0133      P1= .5/A*(-E+D)
0134      P2= F/P1/A
0135      P1= CSQRT(P1)
0136      P2= CSQRT(P2)
0137      WRITE (6,509)
0138      WRITE (6,506) P1,P2
0139      204 WRITE (6,508) CLAP
0140      N2= N/2+1
0141      M2= M/2+1
0142      IF (NTEST.EQ.1) GO TO 211
0143      211 IF (NSTRIP.EQ.1) WRITE (6,514)
0144      C*** GENERATE THE TRANSFORMED EXPRESSIONS
0145      REWIND 2
0146      DO 1 I= 1,N
0147      DK1= 2.*XK/N*(I-.5)-XK
0148      DO 1 J= 1,M
0149      DK2F=2.*TK/M*(J-.5)-TK
0150      SLAP= CMPLX(CLAP,DK2F)
0151      DK2= -SI*SLAP
0152      IF (NTEST.NE.1) GO TO 201
0153      FG= PI*(1.+CEXP(-SLAP))/(SLAP*SLAP+PI*PI)*
1CSIN(DK1)/DK1*(1.+DK1*DK1/(PI*PI-DK1*DK1))
0154      C*** TEST FOR A STRING
0155      DATA(I,J)=-FG/(SLAP*SLAP+DK1*DK1)
0156      GO TO 1
0157      201 CALL CALCUL(0)
0158      1 CONTINUE
```

FORTRAN IV G LEVEL 21

MAIN

DATE = 74186

11/28/2

```
0154      IF (NTEST.NE.1) GO TO 202
0155      WRITE (6,507)
0156      CALL FOURT (DATA,NN,2,1,1,0)
0157      DO 15 KI= 1,N2
0158      B= -SI*PI/N*(N-1)*(KI-1)
0159      DO 15 KJ= 1,M
0160      C= -SI*PI/M*(M-1)*(KJ-1)
0161      T= PI/TK*(KJ-1)
0162      DATA (KI,KJ)= DATA (KI,KJ)*XK*TK/PI/PI/N/M*CEXP (B)*CEXP (C)
0163      15 DATA (KI,KJ)= DATA (KI,KJ)*EXP (CLAP*T)
0164      WRITE (6,506) ((DATA (I,J), J= 1,M), I= 1,N2)
0165      GO TO 203
C***** ****
C*** MAIN LOOP FOR DIFFERENT DEPTHS X3
0166      202 DO 6 K3= 1,NK3
0167      X3= (K3-1)*DX3
C*** LOOP FOR CALCULATING DISPLACEMENTS AND STRESSES AT A GIVEN DEPTH
0168      DO 4 K= 1,NP
0169      WRITE (6,680)
0170      WRITE (6,501) X3
0171      REWIND 2
0172      DO 7 I= 1,N
0173      DO 7 J= 1,M
0174      READ (2) P1,P2,C1,C2,S1,S2,DK1,DK2
0175      B= CEXP (-X3*P1)
0176      C= CEXP (-X3*P2)
C*** DISPLACEMENTS
0177      IF (K.EQ.1) DATA (I,J)= C1*B+C2*C
0178      IF (K.EQ.2) DATA (I,J)= C1*S1*B+C2*S2*C
C*** STRESSES
0179      IF (K.EQ.3)
1DATA (I,J)= (C13*SI*DK1-C33*P1*S1)*C1*B+ (C13*SI*DK1-C33*P2*S2)*C2*C
0180      IF (K.EQ.4)
1DATA (I,J)= (C11*SI*DK1-C13*P1*S1)*C1*B+ (C11*SI*DK1-C13*P2*S2)*C2*C
0181      IF (K.EQ.5)
1DATA (I,J)= C55*((-P1+SI*DK1*S1)*C1*B+ (-P2+SI*DK1*S2)*C2*C)
0182      IF (K.LT.6) GO TO 7
C*** DISPL. FOR A BEAM ON AN ELASTIC FOUNDATION
0183      EF=0.1
C*** FORCING FUNCTION
0184      FG= FI*FG1*(1.+CEXP (-SI*DK2*T0))/(PI*PI-DK2*DK2*T0*T0)*
14./(DK1*A0)**2*(CSIN (DK1*A0)/DK1-A0*CCOS (DK1*A0))
0185      D=W*EK1*DK1/12.0*(ES*W*W*DK1*DK1-RO*W*W*DK2*DK2)-RO*W*DK2*DK2
1+EF
0186      IF (K.EQ.6)
1DATA (I,J)=FG/D
7 CONTINUE
0187      CALL FOURT (DATA,NN,2,1,1,0)
0188      DO 3 KI= 1,N2
0189      B= -SI*PI/N*(N-1)*(KI-1)
0190      DO 3 KJ= 1,M
0191      C= -SI*PI/M*(M-1)*(KJ-1)
0192      T= PI/TK*(KJ-1)
0193      DATA (KI,KJ)= DATA (KI,KJ)*XK*TK/PI/PI/M/N*CEXP (B)*CEXP (C)
0194      E= CLAP*T
0195
0196      3 DATA (KI,KJ)= DATA (KI,KJ)*EXP (E)
```

FORTRAN IV G LEVEL 21

MAIN

DATE = 74186

11/28/2

C*** CALCULATE THE PHOTOLELASTIC FRINGE ORDER
0197 DO 290 I=1,40
0198 DO 290 J=1,32
0199 IF (K.EQ.3) T33(I,J)=REAL(DATA(I,J))
0200 IF (K.EQ.4) T11(I,J)=REAL(DATA(I,J))
0201 IF (K.EQ.5) T13(I,J)=REAL(DATA(I,J))
0202 IF (K.EQ.5) GO TO 280
0203 GO TO 290
0204 280 CONTINUE
0205 FNGE=(T11(I,J)-T33(I,J))**2+4.0*T13(I,J)*T13(I,J)
0206 FRNGE(I,J)=SQRT(FNGE)
0207 290 CONTINUE
0208 214 WRITE (6,511) K
C*** FIND THE MAXIMUM VALUE
0209 RS= 1.E-3
0210 DO 14 I=1,40
0211 DO 14 J= 1,32
0212 S= DATA(I,J)
0213 TP= REAL(S)/RS
0214 IF (ABS(TP).LT.1.) GO TO 14
0215 RS= REAL(S)
0216 14 CONTINUE
0217 WRITE (6,516) RS
C PRINT REAL PART OF DISPL. AND STRESSES
0218 NIJ=N/4
0219 NIJ=10
0220 DO 310 I=1,NIJ
0221 I1=I-1
0222 WRITE(6,600) I1
0223 DO 300 J=1,32
0224 SR=REAL(DATA(I,J))/RS
0225 SIMG=AIMAG(DATA(I,J))/RS
0226 RDATA(J)=SR
0227 CIDATA(J)=SIMG
0228 300 CONTINUE
0229 WRITE(6,620) (RDATA(L),L=1,M)
0230 WRITE(6,650)
0231 WRITE(6,620) (CIDATA(L),L=1,11)
0232 310 CONTINUE
0233 WRITE(6,680)
0234 IF (K.EQ.1) WRITE(6,630)
0235 IF (K.EQ.2) WRITE(6,631)
0236 IF (K.EQ.3) WRITE(6,632)
0237 IF (K.EQ.4) WRITE(6,633)
0238 IF (K.EQ.5) WRITE(6,634)
0239 IF (K.EQ.6) WRITE(6,635)
0240 WRITE(6,640) DX,DT
C*** PLOT THE RELATIVE VALUES
0241 DO 12 J= 1,M
0242 DO 13 I=1,40
0243 S= DATA(I,J)
0244 13 MM(I)= REAL(S)/RS*100
0245 WRITE (6,515) MM
0246 12 CCNTINUE
C*** PLOT A MAP OF PHOTOLELASTIC FRINGE ORDER
0247 IF (K.LT.5) GO TO 4

FORTRAN IV G LEVEL 21

MAIN

DATE = 74186

11/28/2

```
0248      RS=1.E-3
0249      DO 312 I=1,20
0250      DO 312 J=1,20
0251      SS=FRNGE(I,J)
0252      TP=SS/RS
0253      IF (ABS(TP).LT.1.) GO TO 312
0254      RS=SS
0255 312 CONTINUE
0256      WRITE(6,680)
0257      WRITE(6,516) RS
0258      WRITE(6,690)
0259      DO 320 J=1,32
0260      DO 315 I=1,40
0261      SS=FRNGE(I,J)
0262      315 MM(I)=SS/RS*100
0263      WRITE(6,515) MM
0264 320 CONTINUE
0265      4 CONTINUE
0266      6 CONTINUE
0267      100 FORMAT (8E10.4)
0268      101 FORMAT (2I5,3F10.3)
0269      102 FORMAT (3I5)
0270      490 FORMAT(5X,55H ELASTIC CONSTANTS C11,C22,C33,C44,C55,C66,C12,C13,C3
12,/9E12.4,/)
0271      491 FORMAT(5X,25H DENSITY OF PLATE GM/CC--,F10.4,5X,20H FIBER LAYUP AN
1GLE--,F10.4)
0272      500 FORMAT (2F12.4,4E15.4)
0273      501 FORMAT (5H X3= F10.4)
0274      502 FORMAT (10H STRESSES I3/(8E15.7))
0275      503 FORMAT (5X5H DATA, 15X10HCONSTANTS ,20X10HPARAMETERS /8E15.7)
0276      504 FORMAT (5X8HNSTRESS= I3,5X4HNX3= I4,5X4HDX3= F10.4,/)
0277      505 FORMAT (14H SIMPLE POLES )
0278      506 FORMAT (8E15.7)
0279      507 FORMAT (15H THIS IS A TEST )
0280      508 FORMAT (30H LAPLACE INVERSION PARAMETER= F12.4)
0281      509 FORMAT (28H SECCND ORDER BRANCH POINTS )
0282      510 FORMAT(5X,27H LONG.WAVE SPEED IN BEAM = ,F12.3,7H CM/SEC)
0283      511 FORMAT (14H DISPLACEMENTS I4)
0284      512 FORMAT (24H RAYLEIGH SPEED CS/CR*I )
0285      513 FORMAT (8F15.8)
0286      514 FORMAT (/50X 10HWITH STRIP)
0287      515 FORMAT(2X,40I3)
0288      516 FORMAT (16H MAXIMUM VALUE= E15.7)
0289      520 FORMAT(/,5X,23H IMPACT PRESSURE(PSI)= ,E12.4,5X,25H 1/2 CONTACT LE
1NGTH(CM)= ,F12.4,5X,23H IMPACT DURATION(SEC)= ,E12.4,/)
0290      521 FORMAT(/,5X,18H DENSITY OF BEAM= ,F12.4,5X,17H NORM.THICKNESS= ,
1F12.4,5X,15H BEAM MODULUS= ,E12.4)
0291      600 FORMAT(/, 20X,18HNORMALIZED DIST.= ,I4)
0292      620 FORMAT(11F10.5)
0293      621 FORMAT(5X,20H WAVELEN(TIME-SEC)= ,E12.4,5X,20H WAVELEN(DIST-CM )=
1,F12.4,/,5X,23H MAX FREQ NO(NON DIM)= ,F12.4,5X,23H MAX WAVE NO(NC
2N DIM)= ,F12.4,/)
0294      630 FORMAT(30X,16H DISPLACEMENT U1,/)
0295      631 FORMAT(30X,16H DISPLACEMENT U3,/)
0296      632 FORMAT(30X,11H STRESS T33,/)
0297      633 FORMAT(30X,11H STRESS T11,/)
```

ORTRAN IV G LEVEL 21

MAIN

DATE = 74186

11/28/2

```
0298      634 FORMAT(30X,11H STRESS T13,/)
0299      635 FORMAT(30X,41H TEST-DISPL.OF BEAM ON ELASTIC FOUNDATION,/)
0300      640 FORMAT(20X,14H-->> X1, DX= ,F12.4,/,20X,2H 1,/,20X,
1 2H 1,/,20X,2H V,/,20X,2H V,/,20X,9H TIME,DT= ,E12.4,/)
0301      650 FORMAT(10H IMAG PART)
0302      680 FORMAT(1H1)
0303      690 FORMAT(/,20X,17H FRINGE ORDER MAP,/,20X,31H SQRT((T11-T33)**2+4.0*
1T13*T13))
0304      710 FORMAT( 5X,6H VEL= ,F12.4,5X,5H T0= ,F12.4,5X,4H A= ,F12.4,5X,
15H F0= ,F12.4,/)
0305      203 STOP
0306      END
```

FORTRAN IV G LEVEL 21

MAIN

DATE = 74186

11/28/2

C

```
0001      SUBROUTINE CALCUL(NPOLE)
0002      COMMON /MMC/ D,DK1
0003      COMMON /MC/DK2,FG1,T0,C11,C13,C33,C55,RHO,RO,W,ES,NSTRIP,A0
0004      COMPLEX B1,B2
0005      COMPLEX G0,G01,H0,H01,G10,G11,H10,H11
0006      COMPLEX G,H,G1,H1
0007      COMPLEX DK1,DK2,P1,P2,S1,S2,C1,C2,SI,B,C,D ,FG
0008      COMPLEX*16 BS
0009      PI= 3.14159265
0010      SI= CMPLX(0.,1.)
0011      A= C33*C55
0012      B= C33*(RHO*DK2*DK2-C11*DK1*DK1)+C55*(RHO*DK2*DK2-C55*DK1*DK1)+*
1DK1*DK1*(C13+C55)**2
0013      C= (RHO*DK2*DK2-C11*DK1*DK1)*(RHO*DK2*DK2-C55*DK1*DK1)
0014      BS= 1.D0*B*B-1.D0*4.*A*C
0015      D= CSQRT(BS)
0016      P1= .5/A*(-B+D)
0017      P2= C/P1/A
0018      P1= CSQRT(P1)
0019      IF (REAL(P1).LT.0.0.AND.NPOLE.NE.2) P1= -P1
0020      P2= CSQRT(P2)
0021      IF (REAL(P2).LT.0.0.AND.NPOLE.NE.2) P2= -P2
0022      S1= -SI/DK1      /P1/(C13+C55)*(RHO*DK2*DK2-C11*DK1*DK1+C55*P1*P1)
0023      S2= -SI/DK1      /P2/(C13+C55)*(RHO*DK2*DK2-C11*DK1*DK1+C55*P2*P2)
0024      IF (NPOLE.EQ.2) GO TO 201
0025      C*** FORCING FUNCTION
0026      FG= PI*FG1*(1.+CEXP(-SI*DK2*T0))/(PI*PI-DK2*DK2*T0*T0)*
14./(DK1*A0)**2*(CSIN(DK1*A0)/DK1-A0*CCOS(DK1*A0))
0027      201 IF (NSTRIP.EQ.1) GO TO 202
0028      D= (SI*DK1*S1-P1)*(SI*DK1*C13-P2*C33*S2)-(SI*DK1*S2-P2)*(SI*DK1*
1C13-P1*C33*S1)
0029      IF (NPOLE.EQ.2) RETURN
0030      206 C1= FG/D*(SI*DK1*S2-P2)
0031      C2= FG/D*(P1-SI*DK1*S1)
0032      GO TO 203
0033      202 CONTINUE
0034      C*** MATRIX FOR STRIP PROBLEM
0035      B1=W*W*(ES*DK1*DK1-RO*DK2*DK2)*DK1*DK1/12.0-RO*DK2*DK2
0036      E1=W*B1
0037      B2=-W*(ES*DK1*DK1-RO*DK2*DK2)
0038      G10= C55*(SI*DK1*S1-P1)
0039      H10= C55*(SI*DK1*S2-P2)
0040      G11=B2*(1.0+SI*DK1*S1*W/2)
0041      H11=B2*(1.0+SI*DK1*S2*W/2)
0042      G0=- (SI*DK1*C13-P1*S1*C33)
0043      H0=- (SI*DK1*C13-P2*S2*C33)
0044      G01=-SI*DK1*W*G10/2.0 + B1*S1
0045      H01=-SI*DK1*W*H10/2.0 + B1*S2
0046      H1=H10+H11
0047      G1=G10+G11
0048      G=G0+G01
0049      H=H0+H01
0050      D=G10*H0-G0*H10 + (H0*G11+H01*G10-G0*H11-G01*H10)+(H01*G11-H11*G01
1)
0051      IF (NPOLE.EQ.2) RETURN
```

FORTRAN IV G LEVEL 21

CALCUL

DATE = 74186

11/28/2

0050 C1= -FG/D*H1
0051 C2= FG/D*G1
0052 203 WRITE (2) P1,P2,C1,C2,S1,S2,DK1,DK2
0053 RETURN
0054 END

ELASTIC CONSTANTS C11,C22,C33,C44,C55,C66,C12,C13,C32,
 0.2456E 08 0.1170E 07 0.1374E 07 0.3552E 06 0.2310E 07 0.3552E 06 0.4000E 06 0.1986E 07 0.4558E 06
 DENSITY OF PLATE GM/CC-- 1.4400 FIBER LAYUP ANGLE-- 15.0000
 NSTRESS= 1 NX3= 1 DX3= 1.00000
 VEL= 300.0000 T0= 87.3169* A= 1.3342* F0= 1042938.7500
 WAVELEN (TIME-SEC)= 0.3500E-05 WAVELEN (DIST-CM)= 0.6667
 MAX FREQ NO(NON DIM)= 13.7654 MAX WAVE NO(NON DIM)= 9.4248

C11 = 0.2442E 08 C33 = 0.1196E 07 C55 = 0.2310E 07 C13 = 0.1830E 07

LCNG.SPEED = 0.1081E 07 SHEAR SPEED = 0.3326E 06
 RAYLEIGH SPEED = 0.3020E 06 CR/CS = 0.90800 12
 DENSITY OF BEAM= 2.7000 NORM. THICKNESS= 0.5000 BEAM MODULUS= 0.1124E 08
 LCNG. WAVE SPEED IN BEAM = 535757.750 CM/SEC
 SECOND ORDER BRANCH POINTS 0.1997043E 02 0.0 0.0 0.2266004E 01
 LAPLACE INVERSION PARAMETER= 0.5948
 WITH STRIP

* This program has test cards (#51, 52) to override the Hertz calculation. T0=3510⁻⁶ S A=1 CM.

STRESS T33

-->> x1, DX= 0.3333

1

TIME.DT = 0:1750E-05

X3= 0.0
 DISPLACEMENTS 3
 MAXIMUM VALUE= -0.7104896E 00

		NORMALIZED DIST.=	0	0.41184	0.54907	0.67705	0.78714	0.87790	0.94377	0.98577
0.00050	0.03979	0.14142	0.27084	0.80461	0.70045	0.57593	0.43953	0.28894	0.13502	0.01142
1.00000	0.98948	0.95134	0.89048	-0.06042	-0.06357	-0.03818	-0.05201	-0.01223	-0.05377	
-0.04267	-0.07263	-0.07276	-0.07738							
IMAG PART										
0.00000	-0.00000	0.00000	0.00000	0.00000	0.00001	0.00001	0.00002	0.00001	0.00002	0.00003
		NORMALIZED DIST.=	1	0.36748	0.49373	0.61244	0.71537	0.80083	0.86362	0.90441
0.00052	0.03504	0.12364	0.23925	0.74692	0.65225	0.53870	0.41383	0.27579	0.13423	0.01894
0.91968	0.91198	0.87880	0.82442	-0.06060	-0.06261	-0.03975	-0.05059	-0.01542	-0.04968	
-0.03628	-0.06768	-0.07048	-0.07543							
IMAG PART										
0.00000	-0.00000	0.00000	0.00000	0.00000	0.00001	0.00001	0.00002	0.00001	0.00002	0.00003
		NORMALIZED DIST.=	2	0.24997	0.34647	0.44004	0.52356	0.59467	0.64909	0.68662
0.00046	0.02177	0.07726	0.15621	0.64749	0.59235	0.52308	0.43886	0.34489	0.24037	0.13188
0.70461	0.70446	0.68451	0.64749	-0.06962	-0.06054	-0.06012	-0.04359	-0.04736	-0.02317	0.03829
-0.01809	-0.05320	-0.06323	-0.06323							
IMAG PART										
0.00000	0.00000	0.00000	0.00000	0.00000	0.00000	0.00001	0.00001	0.00001	0.00002	0.00002
		NORMALIZED DIST.=	3	0.11326	0.17235	0.23427	0.29336	0.34651	0.39036	0.42373
0.00028	0.00689	0.02688	0.06236	0.40525	0.36662	0.31768	0.26100	0.19681	0.12822	0.06182
0.44479	0.45370	0.44958	0.43352	-0.06009	-0.05857	-0.05702	-0.04745	-0.04482	-0.03114	0.03385
0.00870	-0.03042	-0.04999	-0.04999							
IMAG PART										
0.00000	0.00000	0.00000	0.00000	0.00000	0.00000	0.00000	0.00001	0.00001	0.00001	0.00001
		NORMALIZED DIST.=	4	0.02457	0.05280	0.08844	0.12718	0.16551	0.20047	0.23014
0.00030	0.00089	0.00200	0.00749	0.27493	0.26619	0.25006	0.22685	0.19759	0.16280	0.12382
0.25300	0.26837	0.27564	0.27493	0.04672	-0.05288	-0.05368	-0.04925	-0.04457	-0.03642	-0.03159
0.03868	-0.0176	-0.03008	-0.04672							
IMAG PART										
0.00000	0.00000	-0.00000	-0.00000	0.00000	0.00000	0.00000	0.00000	0.00000	0.00000	0.00000
		NORMALIZED DIST.=	5	-0.01476	-0.00909	0.00649	0.02920	0.05590	0.08350	0.10982
0.00032	0.00039	-0.00267	-0.01052	0.17462	0.17771	0.17551	0.16799	0.15576	0.13895	0.11848
0.13298	0.15198	0.16592	0.17462	-0.0428	-0.02892	-0.04250	-0.04904	-0.04829	-0.03865	-0.03469
0.06546	0.02911	-0.00428	-0.00428							
IMAG PART										
0.00000	0.00000	-0.00000	-0.00000	0.00000	0.00000	0.00000	0.00000	0.00000	0.00000	0.00000

X3 = 0.0
 DISPLACEMENTS 4
 MAXIMUM VALUE = -0.1169061E 01

X3= 0.0
 DISPLACEMENTS 5
 MAXIMUM VALUE= -0.4623035E 00

NORMALIZED DIST.= 0					
0.00000	0.00000	0.00000	0.00000	0.00000	-0.00000
-0.00000	-0.00000	-0.00000	-0.00000	-0.00000	-0.00000
0.00000	0.00000	0.00000	0.00000	0.00000	0.00000
IMAG PART					
0.00000	0.00000	0.00000	0.00000	0.00000	0.00000
NORMALIZED DIST.= 1					
-0.00043	0.02068	0.10175	0.20639	0.30728	0.39631
0.60465	0.58452	0.54925	0.50110	0.43993	0.36875
-0.07283	-0.05896	-0.03786	-0.02592	-0.01095	-0.00946
IMAG PART					
0.00000	-0.00000	0.00000	0.00000	0.00000	0.00000
NORMALIZED DIST.= 2					
-0.00013	0.03502	0.15215	0.31697	0.48494	0.63521
0.99229	0.96012	0.90298	0.82454	0.72472	0.60842
-0.12971	-0.11354	-0.07743	-0.05318	-0.02567	-0.01857
IMAG PART					
0.00000	0.00000	0.00000	0.00000	0.00000	0.00000
NORMALIZED DIST.= 3					
-0.00001	0.02103	0.10073	0.24333	0.41035	0.56703
0.95511	0.92661	0.87394	0.80010	0.70587	0.59526
-0.15673	-0.15637	-0.11853	-0.08225	-0.04707	-0.02788
IMAG PART					
0.00000	0.00000	0.00000	0.00000	0.00000	0.00000
NORMALIZED DIST.= 4					
-0.00004	-0.00297	0.00997	0.07754	0.19345	0.31982
0.67025	0.65479	0.62217	0.57325	0.51049	0.43492
-0.14683	-0.17773	-0.15636	-0.11319	-0.07501	-0.04060
IMAG PART					
0.00000	0.00000	0.00000	0.00000	0.00000	0.00000
NORMALIZED DIST.= 5					
0.00030	-0.00548	-0.02595	-0.02357	0.03348	0.12663
0.45759	0.45334	0.43645	0.40685	0.36774	0.31856
-0.10517	-0.16989	-0.18071	-0.14489	-0.10571	-0.06167
IMAG PART					
0.00000	0.00000	-0.00000	-0.00000	0.00000	0.00000

MAXIMUM VALUE = 0.1168567E 01

PERNGE ORDER MAP

```
SQRT((T11-T33)**2+4.0*T13*T13))
```

JOB 0350 7/5/74 IBM 360-91

EXECUTION TIME 34 SEC.

25 PAGES

CORE 150 K

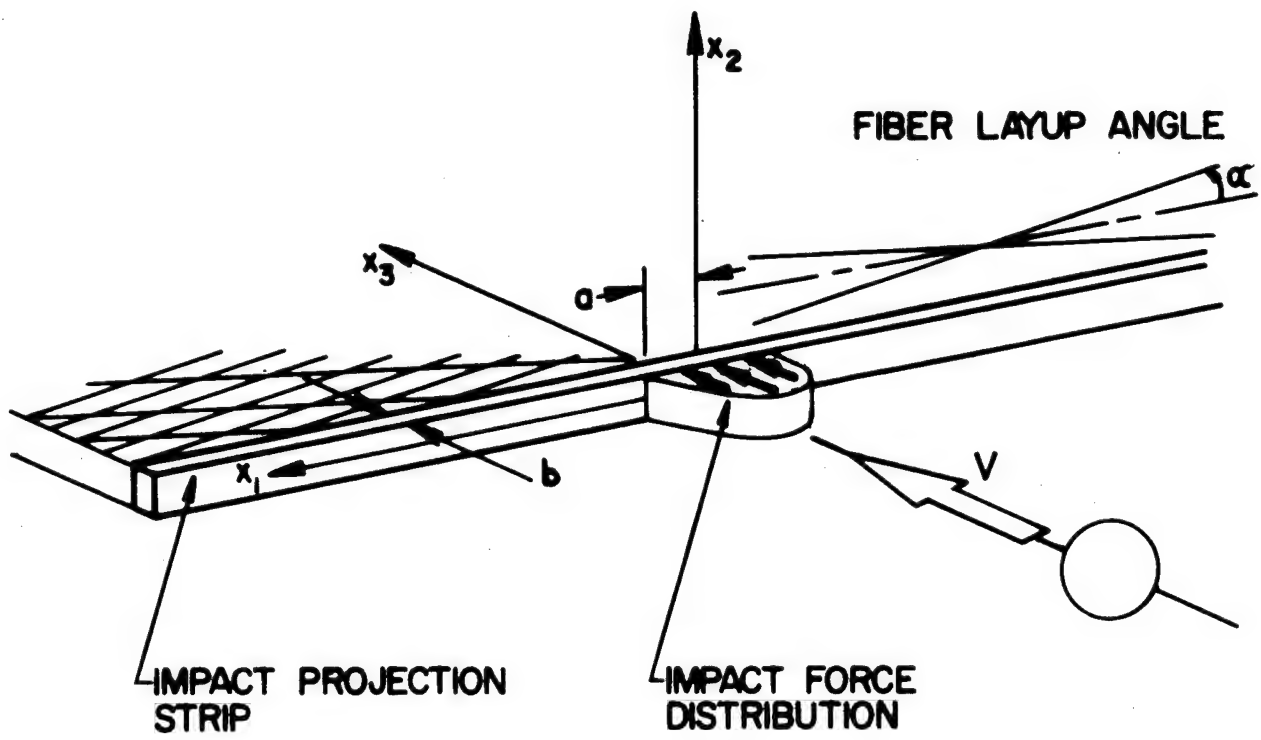


FIGURE 1

GEOMETRY OF IN-PLANE EDGE IMPACT OF
A COMPOSITE PLATE WITH PROJECTION STRIP

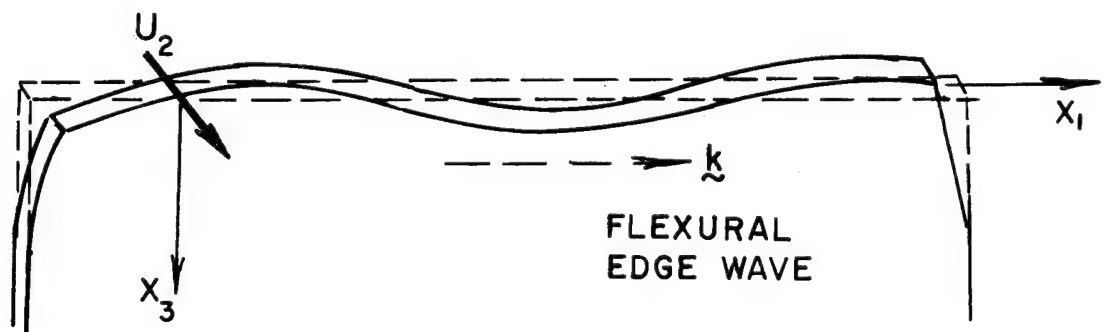
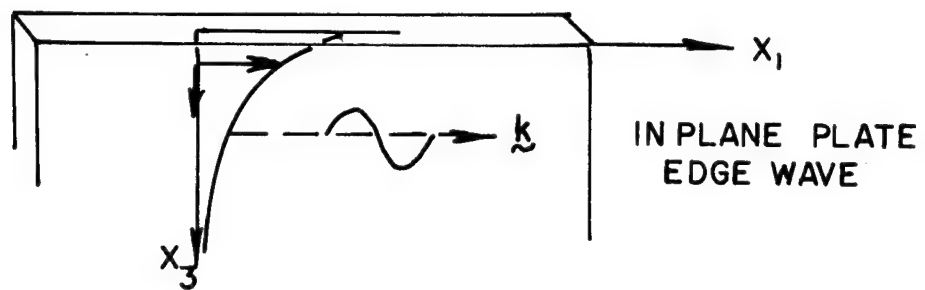
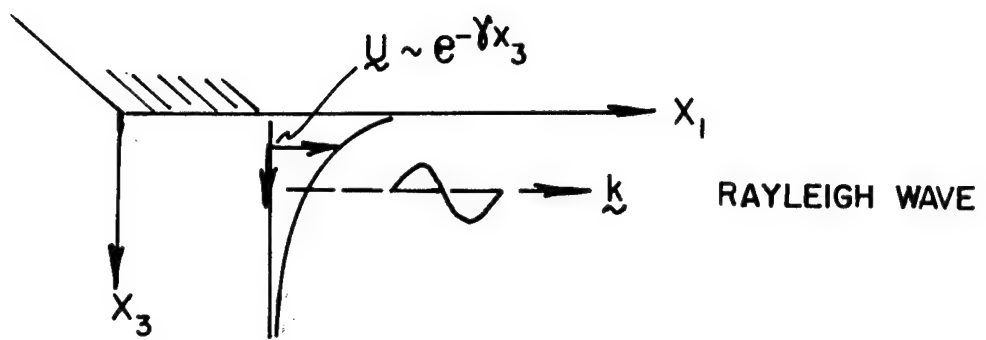


FIGURE 2a

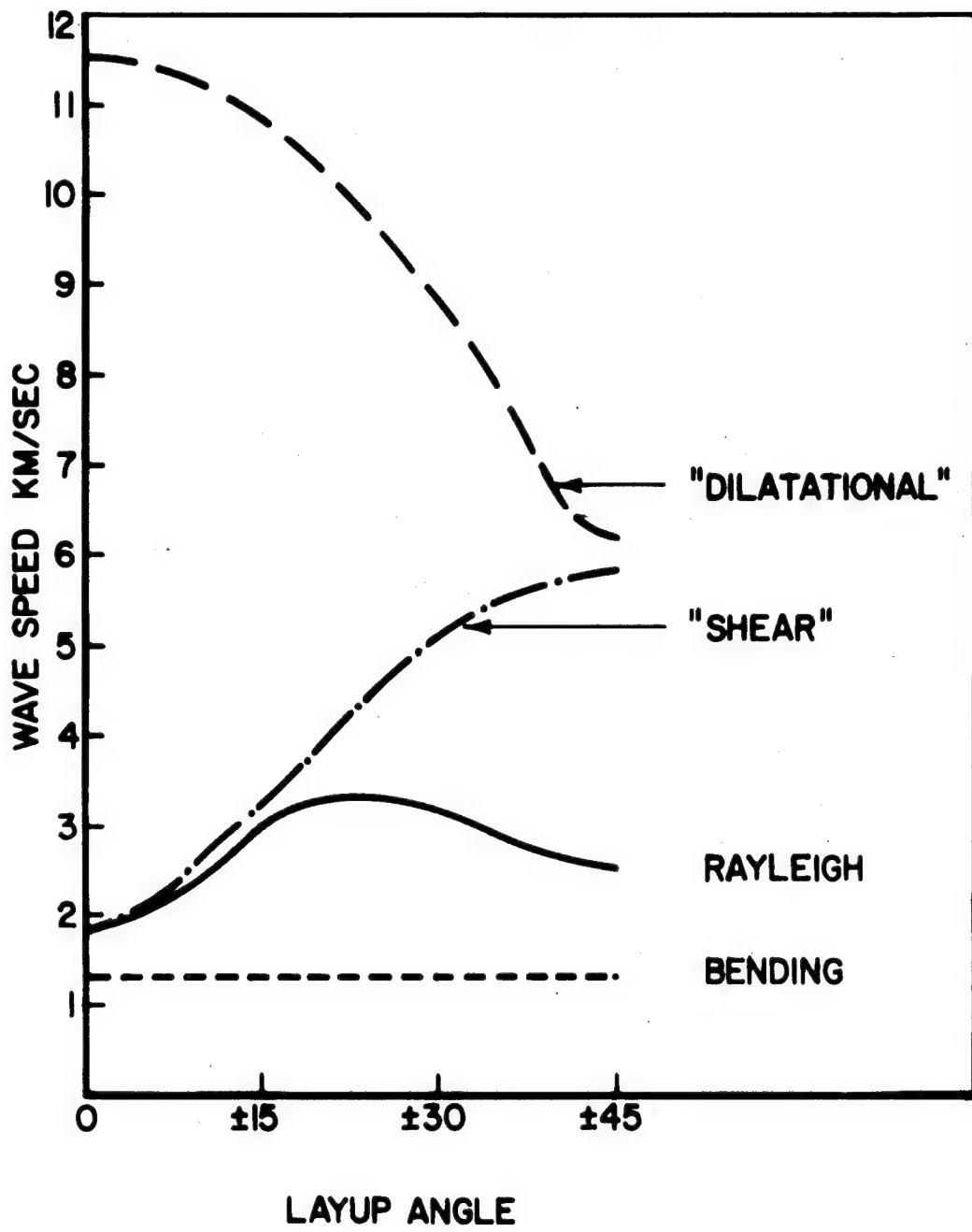


FIGURE 2b

Comparison of In-plane plate edge wave speed with body wave speeds versus fiber layup angle for 55% graphite fiber/epoxy matrix composite.

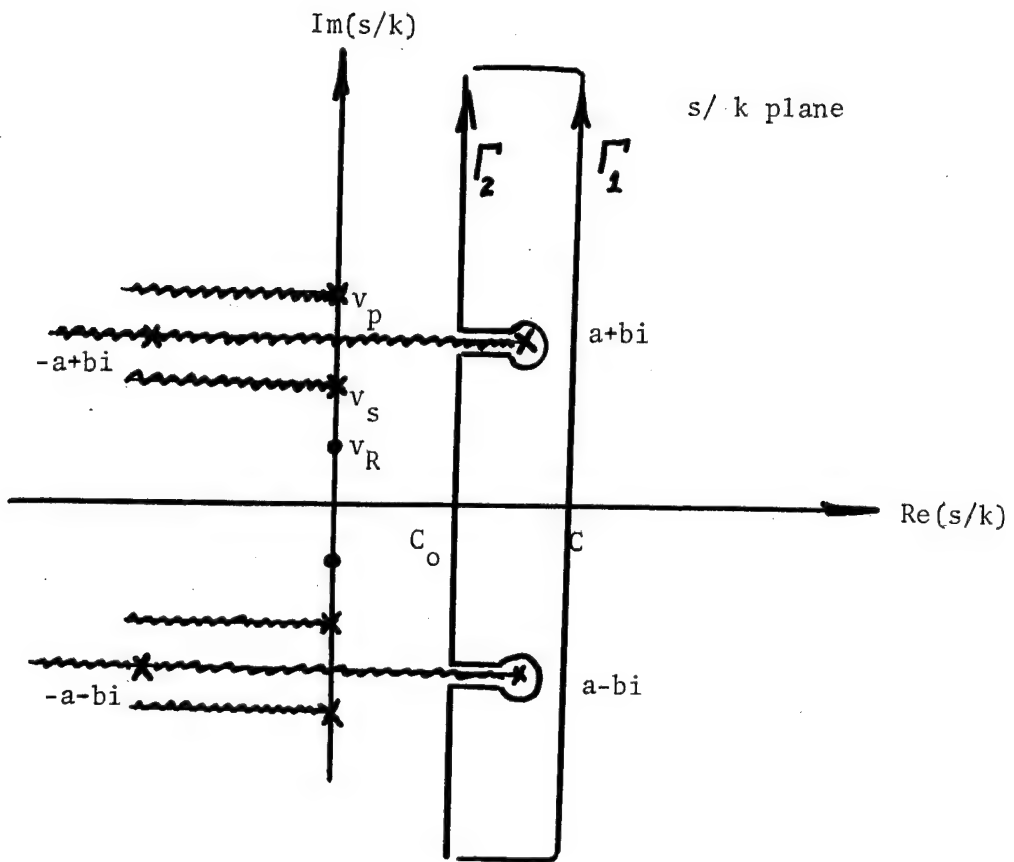


FIGURE 3.

Poles, Branch Points and Integration Contours in the complex Plane for the Numerical Solution.

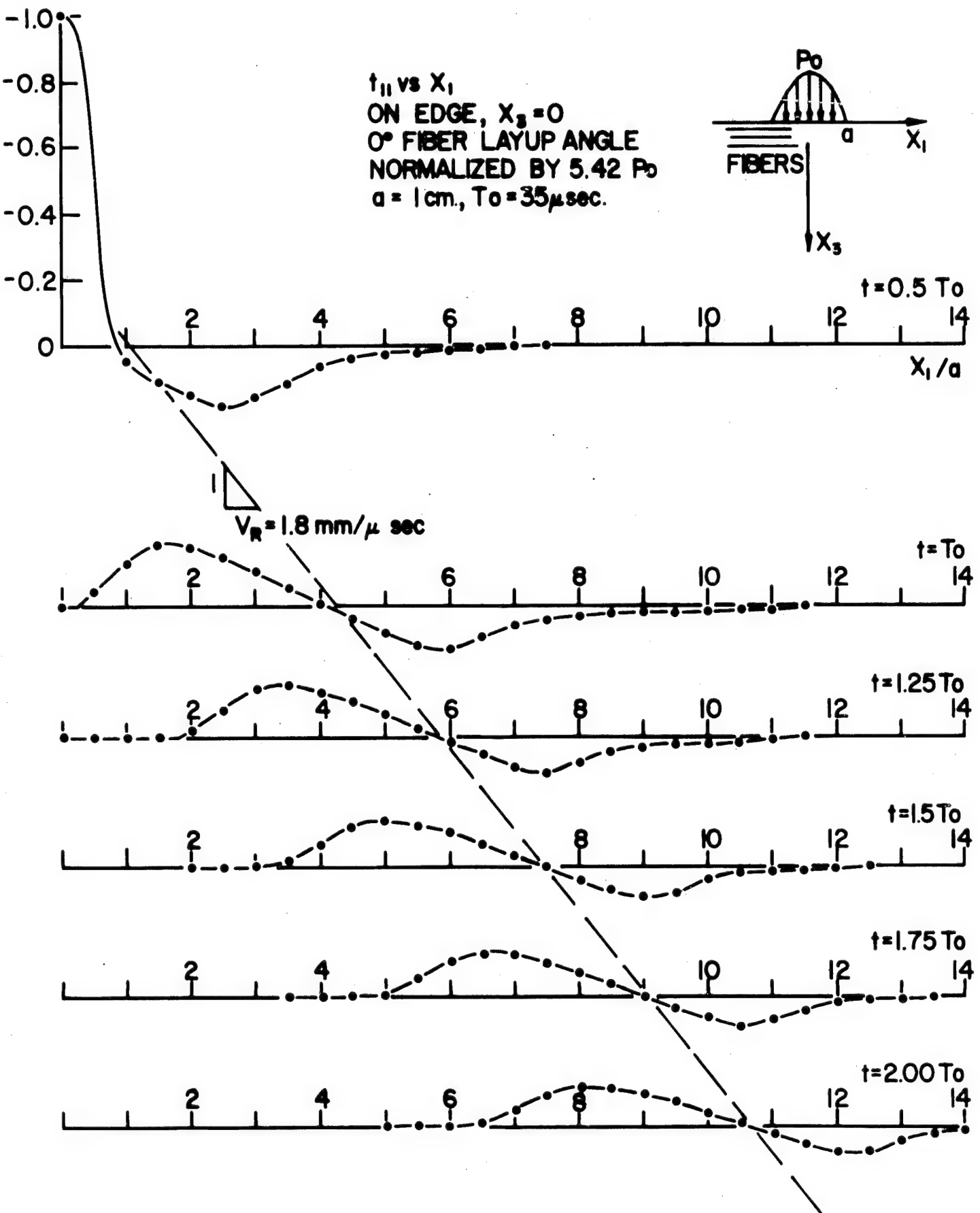


FIGURE 4

Edge Stress t_{11} , Surface Wave for 0° Fiber layup Angle: 55% graphite fiber/epoxy matrix composite

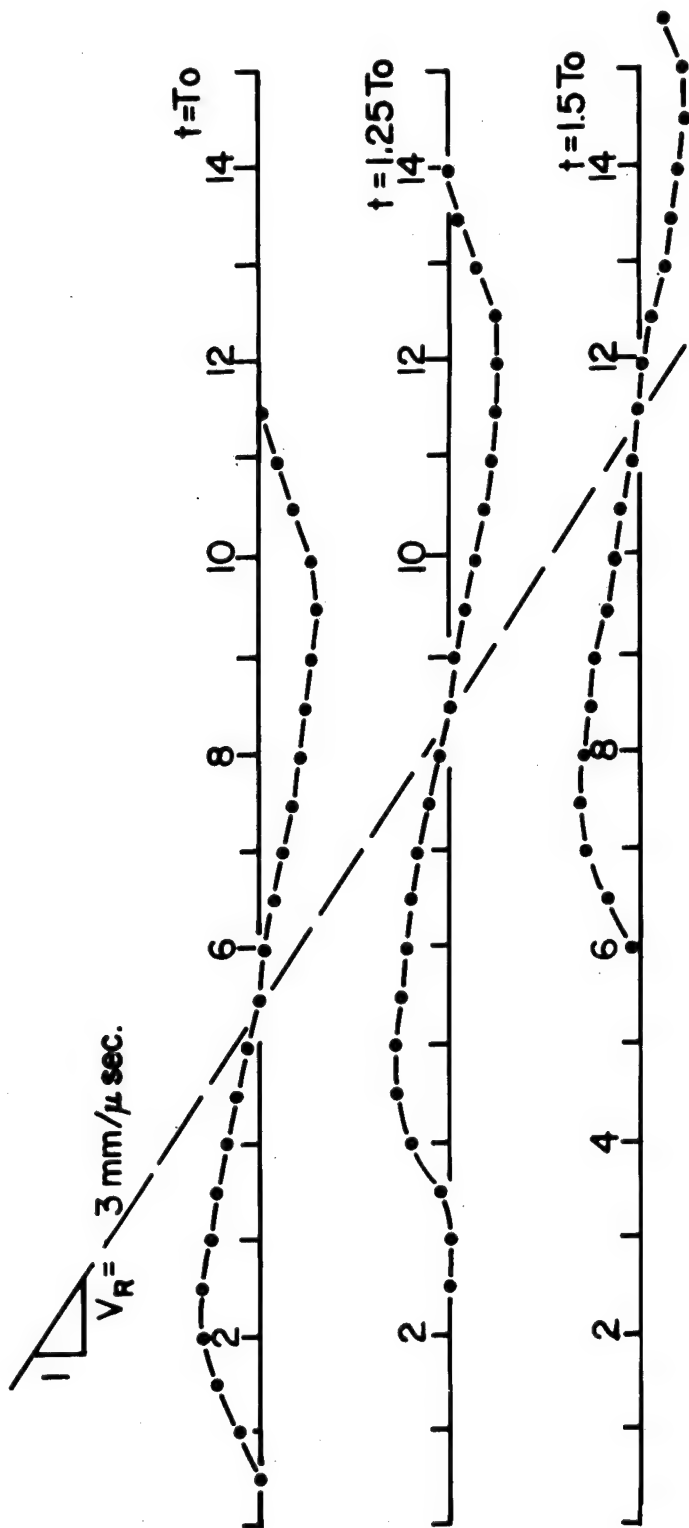
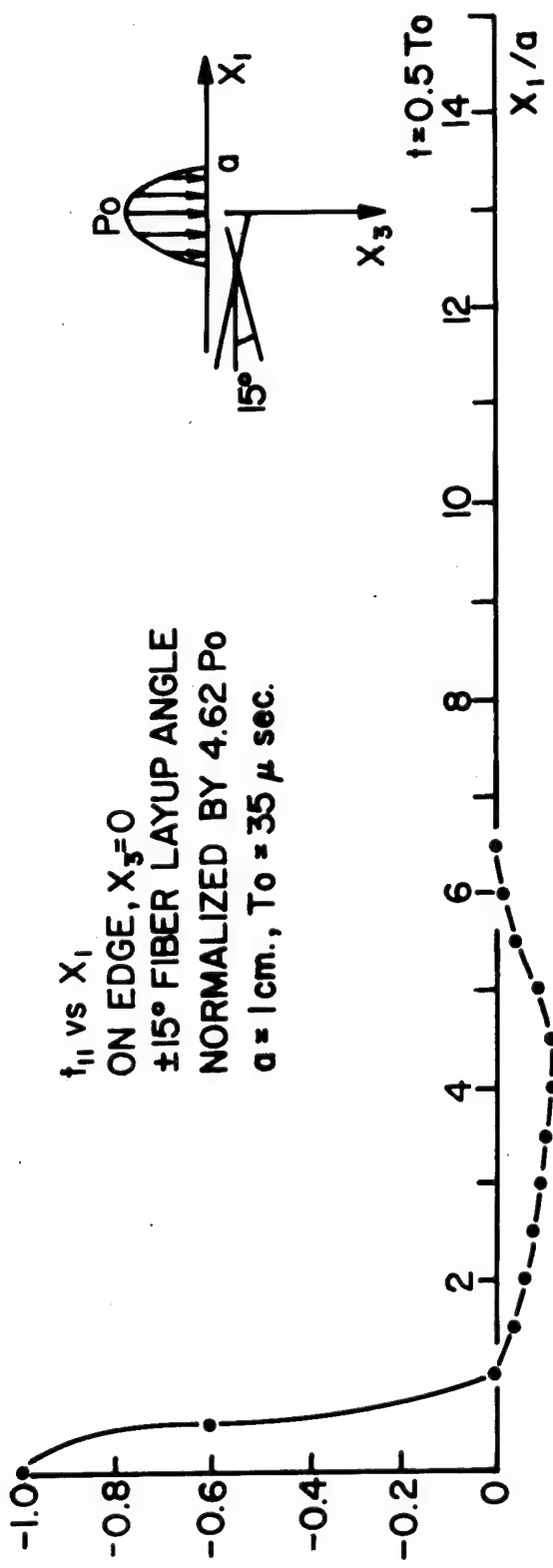


FIGURE 5

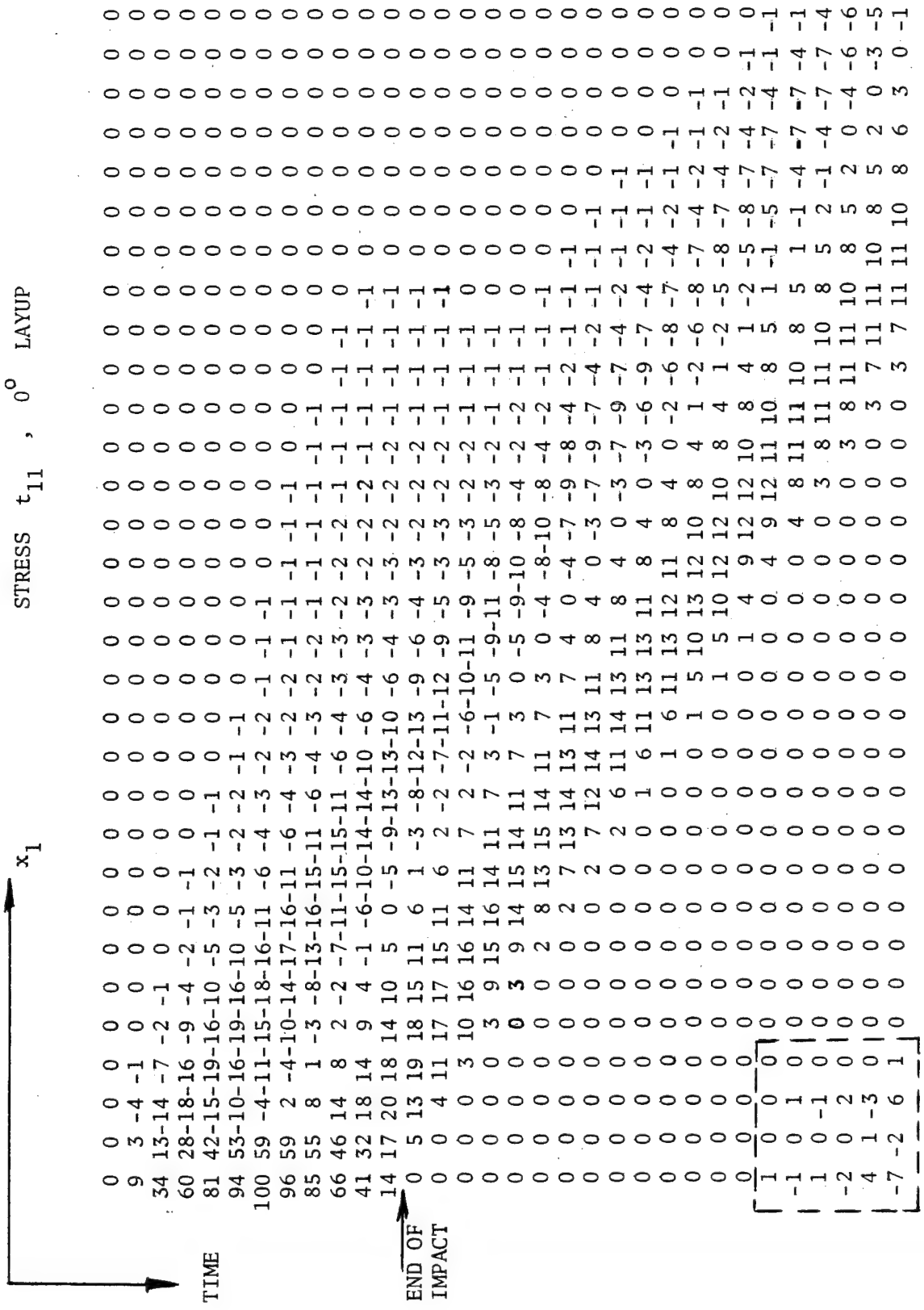
Edge Stress t_{11} Surface Wave for $\pm 15^\circ$ Fiber Layup Angle: 55% Graphite fiber/epoxy matrix composite.

STRESS T33

-->> x1, dx = 0.4447

FIGURE 6

Computer Map of Edge Impact Pressure t_{33} Impact Time 87 μ sec.



Computer Map of Edge Stress t_{11} Surface Wave in the Space-Time (x_1, t) Domain

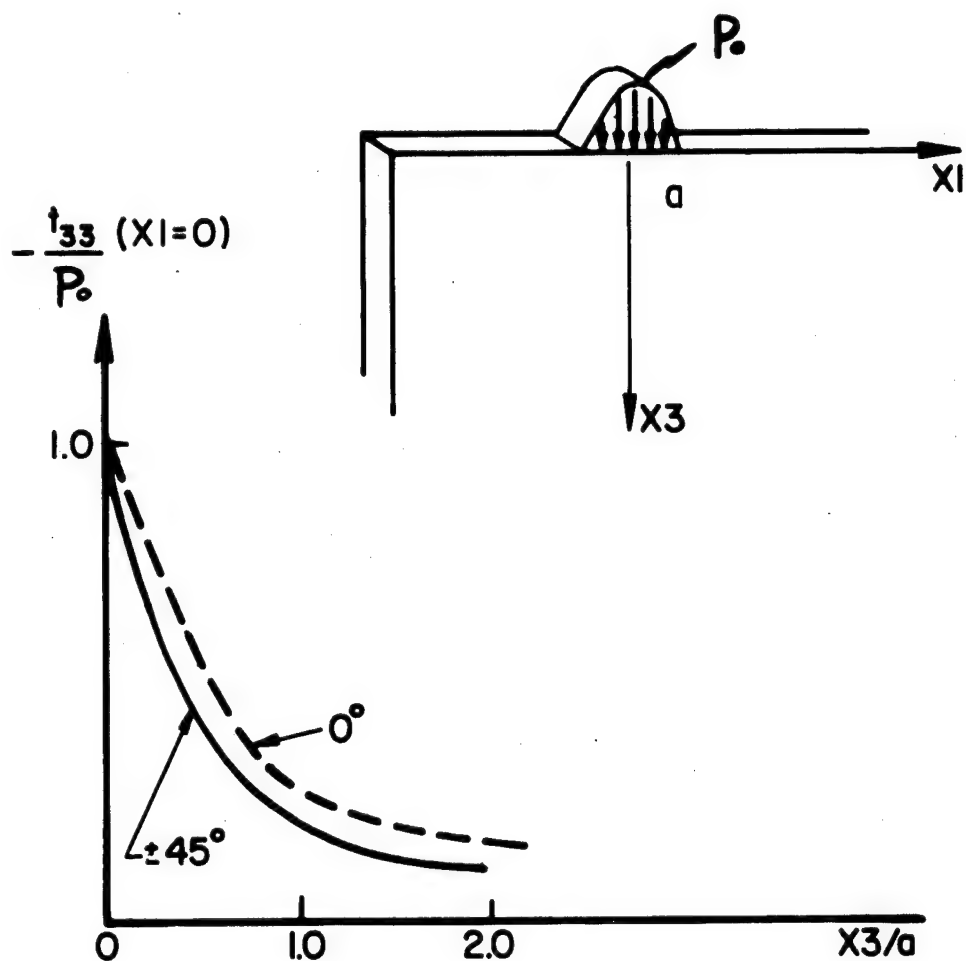


FIGURE 8
Decrease of Stress t_{33} with Distance from the Impact Edge.

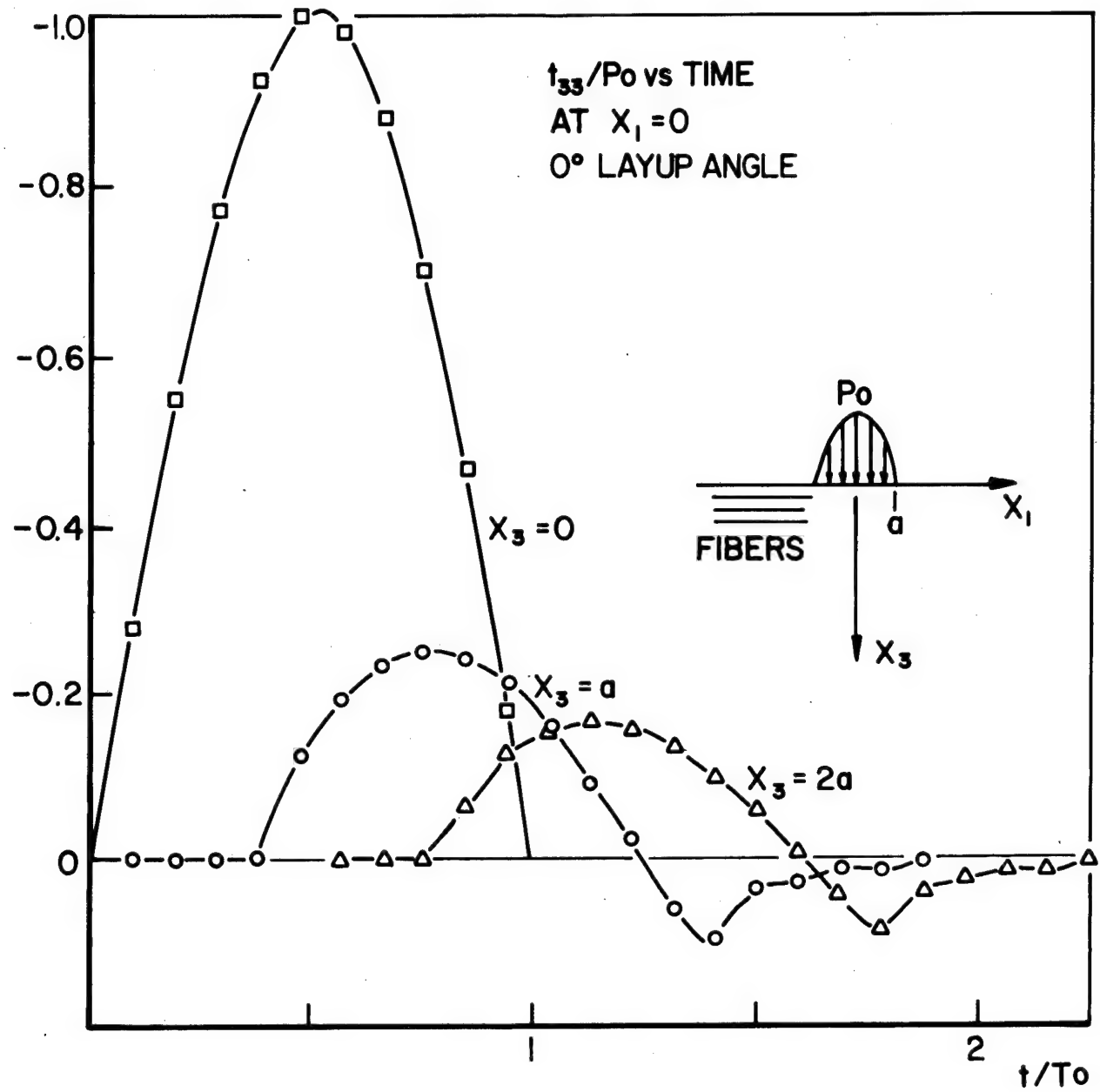


FIGURE 9

Stress t_{33} versus Time at Different Distances from the Edge under the Contact Point.

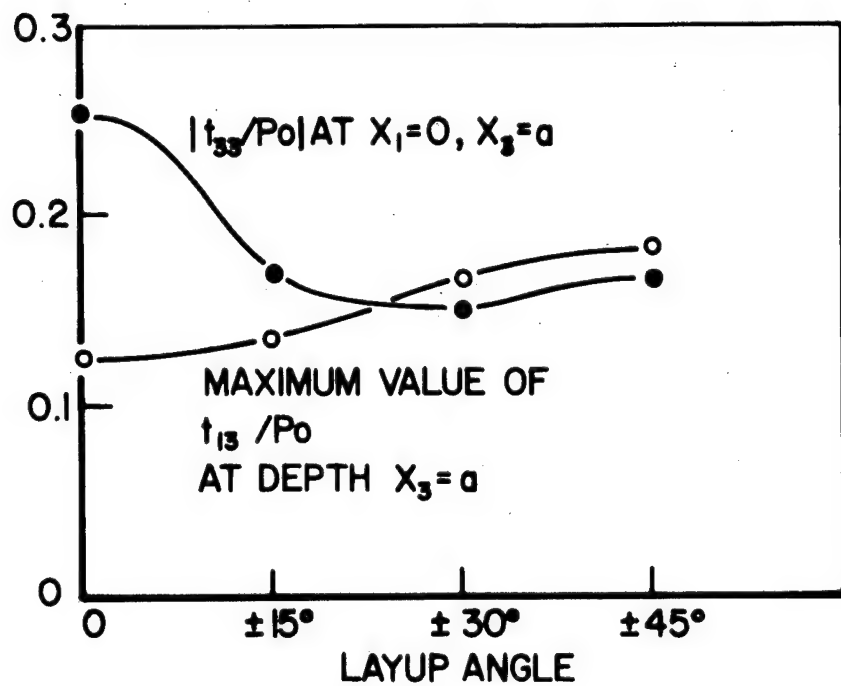
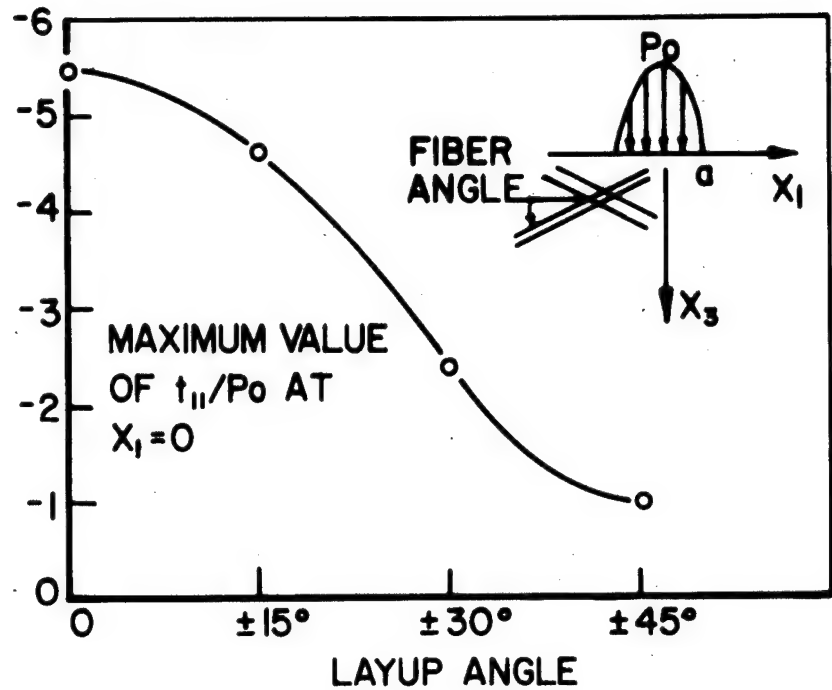


FIGURE 10

Maximum Stresses versus Layup angle for 55% Graphite Fiber/epoxy Matrix Composite.

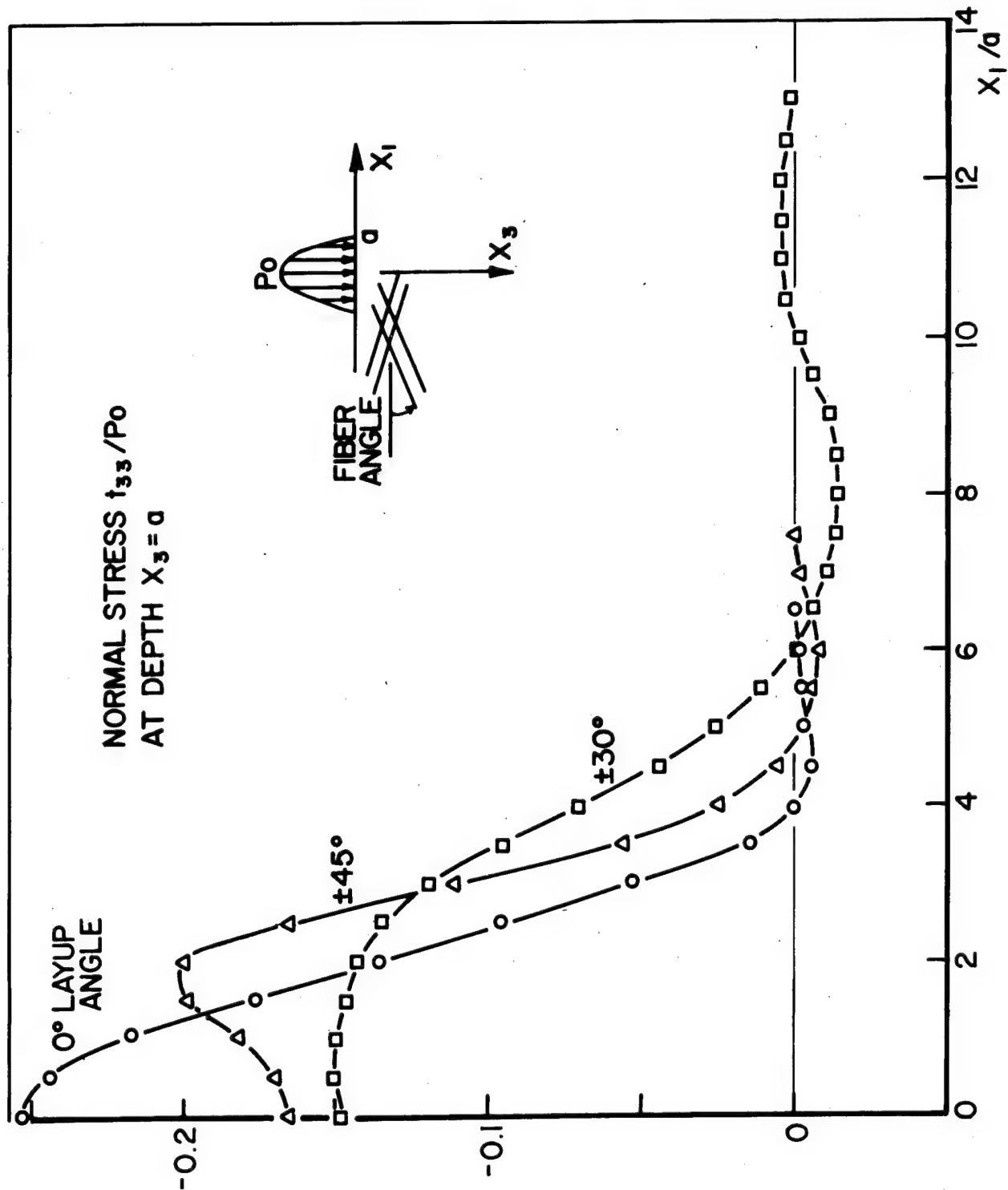
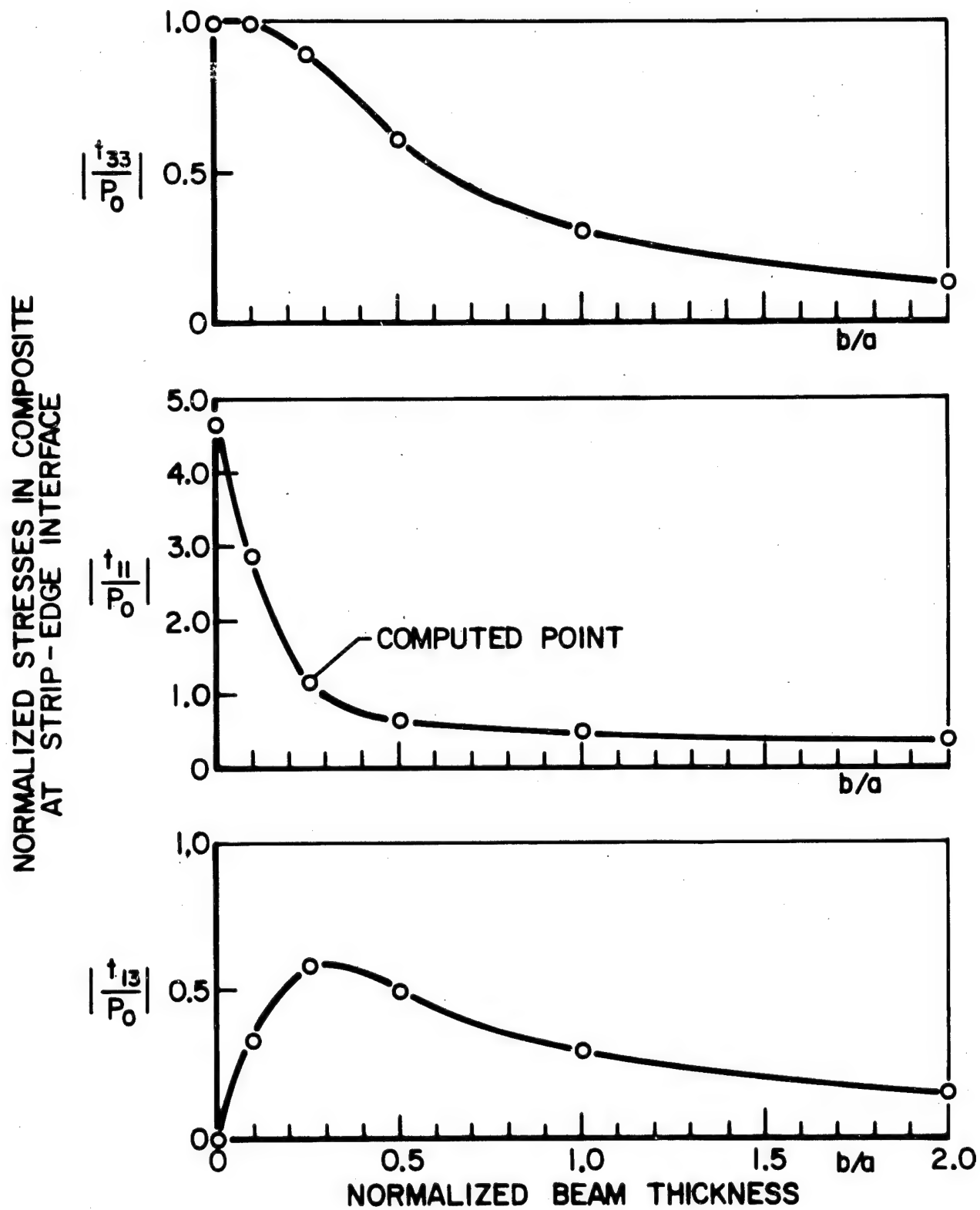


FIGURE 11

Distribution of Stress t_{33} Along the Edge for Fiber Layup angles 0° , $\pm 30^\circ$, $\pm 45^\circ$.

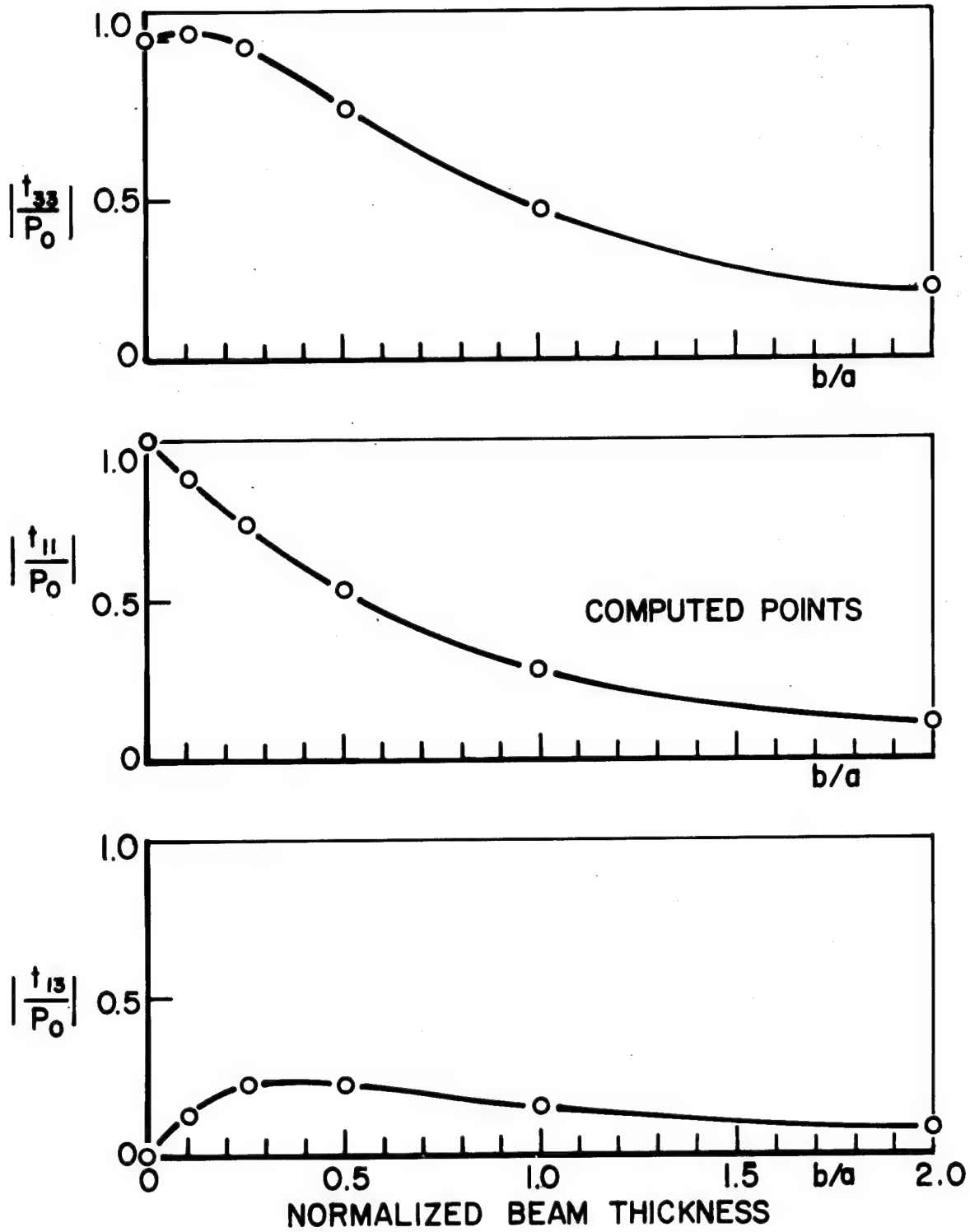


DATA FOR 55% GRAPHITE FIBER/EPOXY MATRIX
 $\pm 15^\circ$ LAYUP - STEEL STRIP

FIGURE 12a

Effect of Edge Strip Thickness on Interface Stresses.

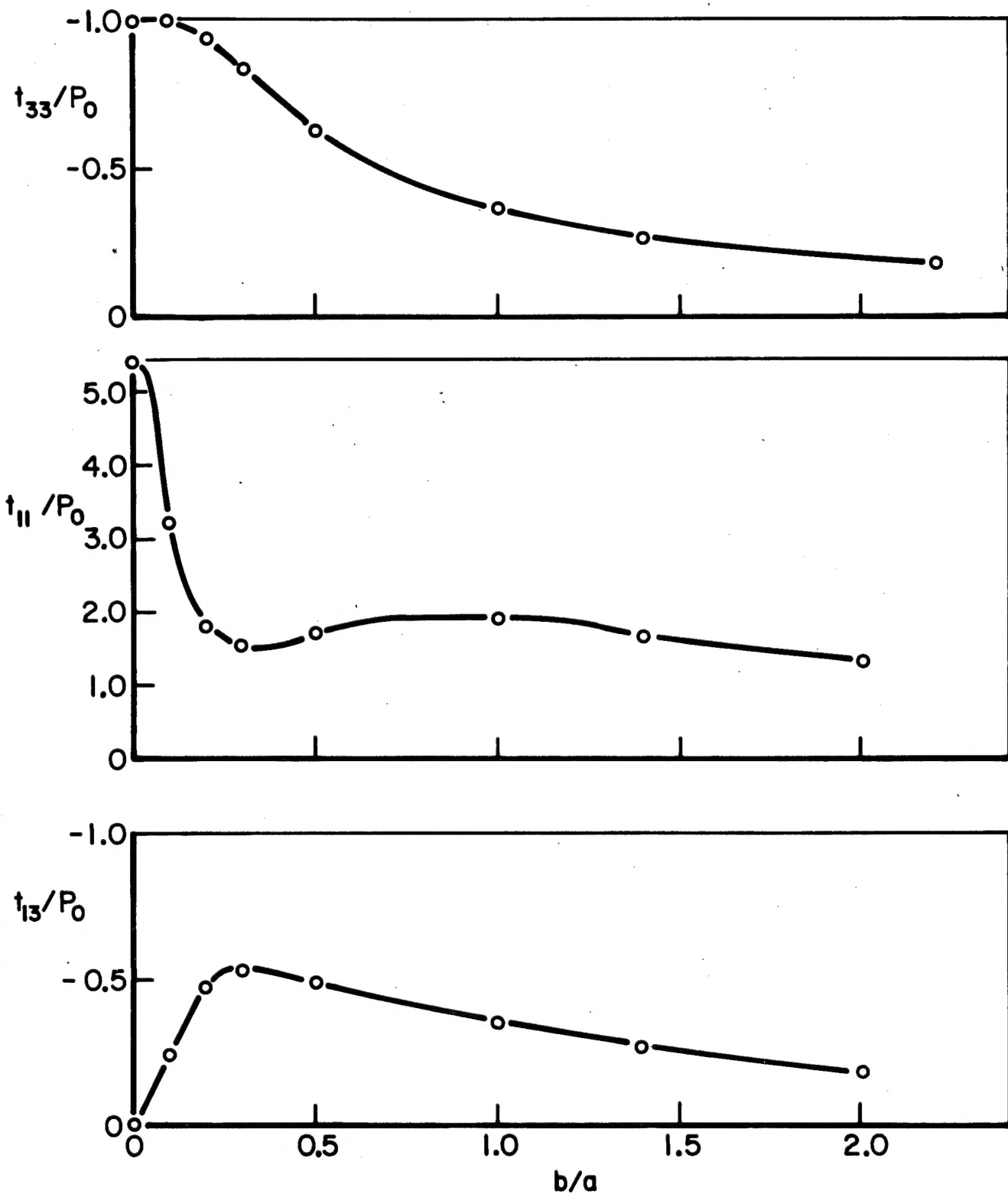
NORMALIZED STRESSES IN COMPOSITE
AT STRIP - EDGE INTERFACE



DATA FOR 55% GRAPHITE FIBER/EPOXY MATRIX
 $\pm 45^\circ$ LAYUP ANGLE - STEEL STRIP

FIGURE 12b

Effect of Edge Strip Thickness on Interface Stresses.



0° LAYUP ANGLE ALUMINUM STRIP

$X_3 = 0$, $a = 1\text{ cm}$, $T_0 = 35\mu\text{sec}$

FIGURE 13

Effect of Edge Strip Thickness on Interface Stresses.

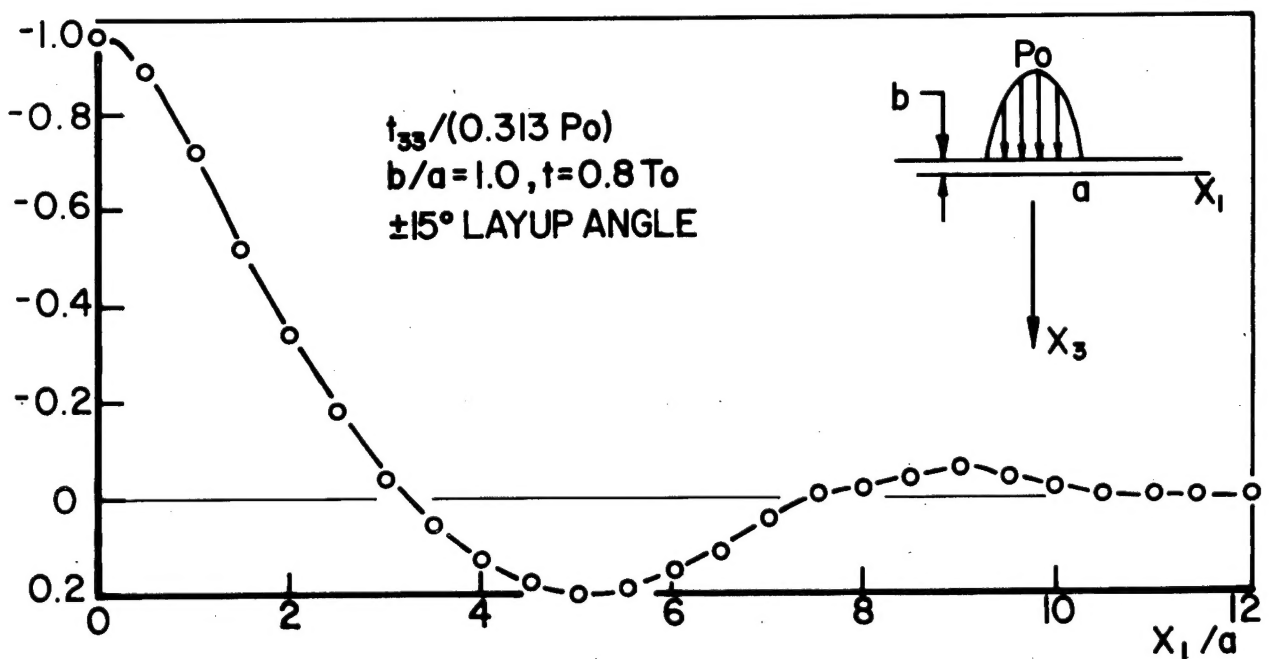
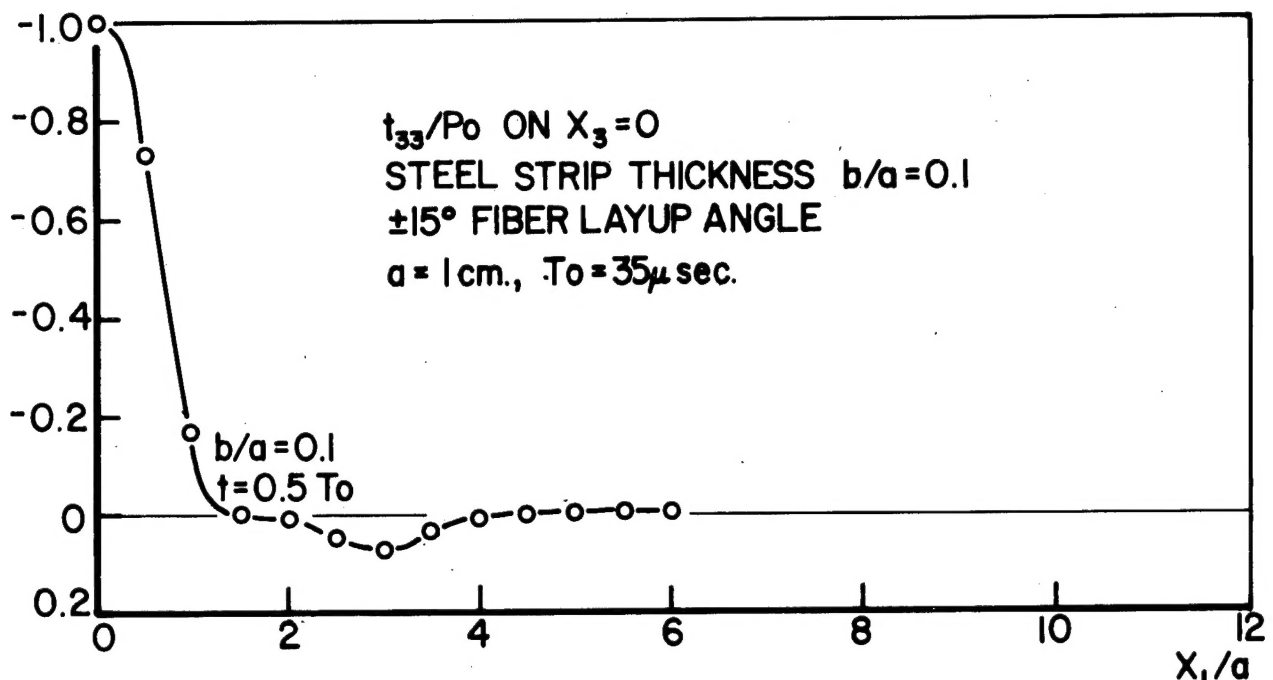


FIGURE 14
 Effect of Edge Strip Thickness on Stress t_{33} Distribution Along the Edge.

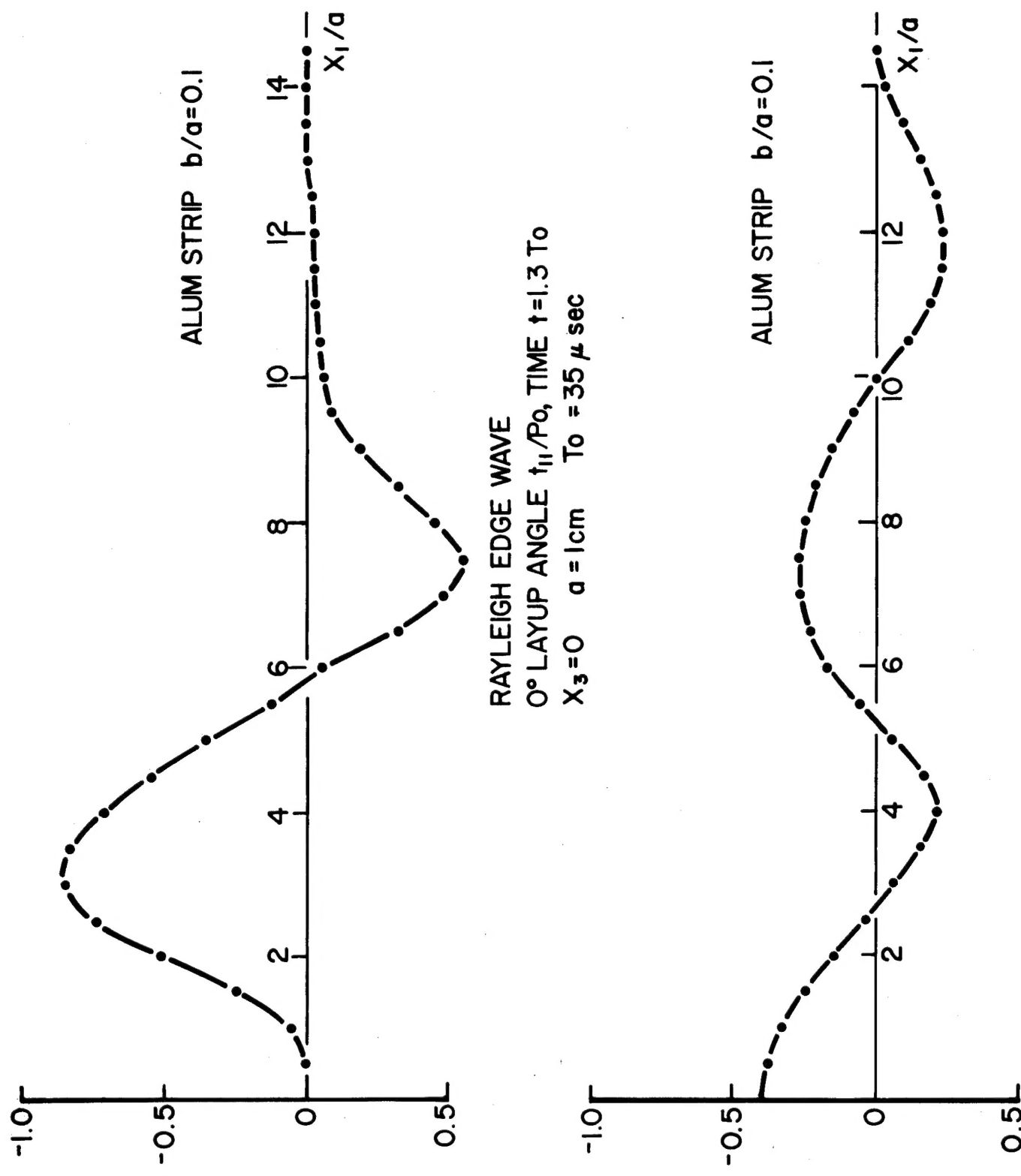


FIGURE 15
Effect of Edge Strip Thickness on the Rayleigh Edge Wave Shape.

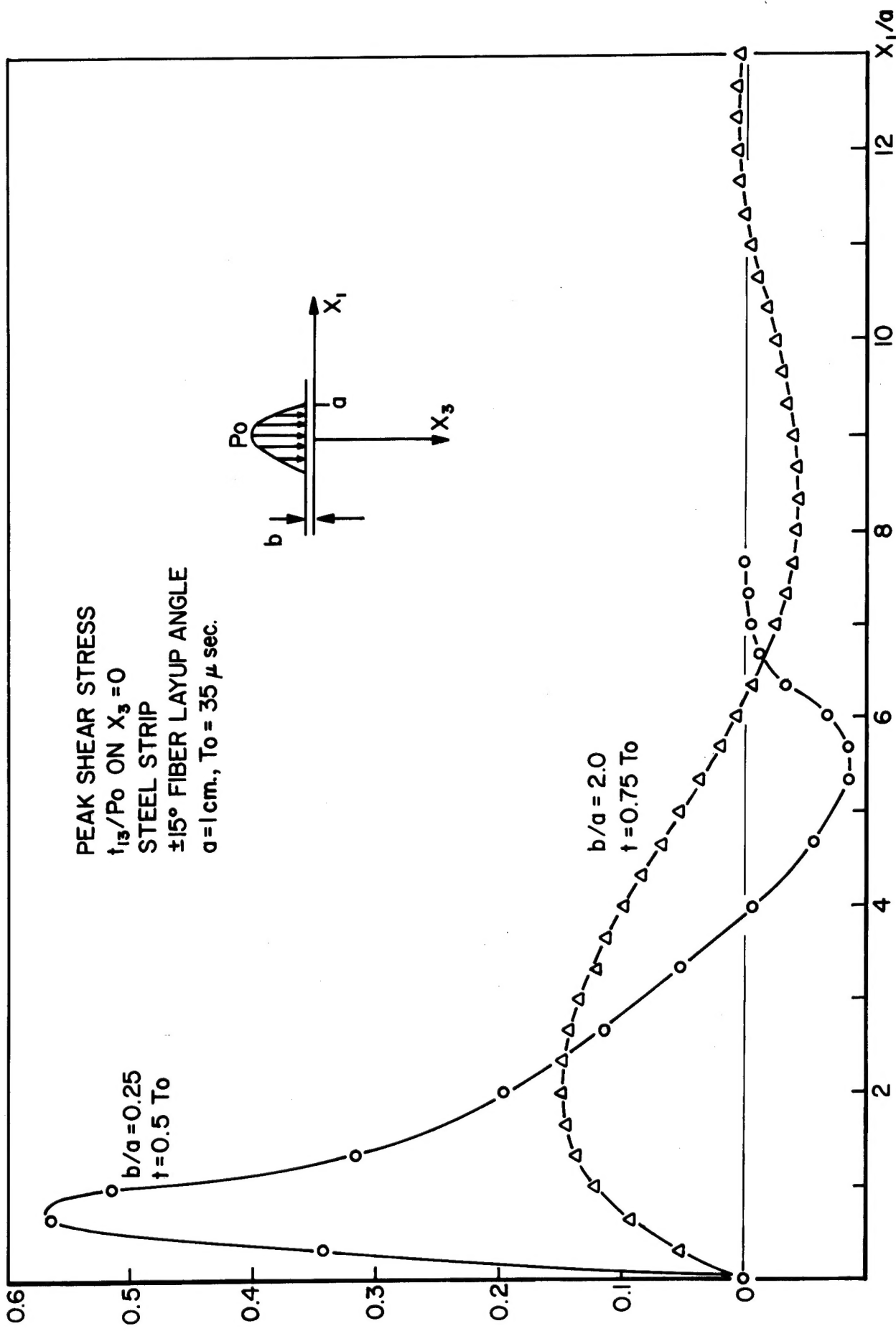


FIGURE 16
Effect of Edge Strip Thickness of Interface Shear Stress t_{13}
Distribution Along the Edge.